AD-A085 170 LA JOLLA INST CA F/6 15/6
DEMOGRAPHICS AND CASUALTY PREDICTION/ANALYSIS.(U)
FEB 80 J J SHEA DCPA01-79-C-0244
UNCLASSIFIED LJI-R-80-060 NL

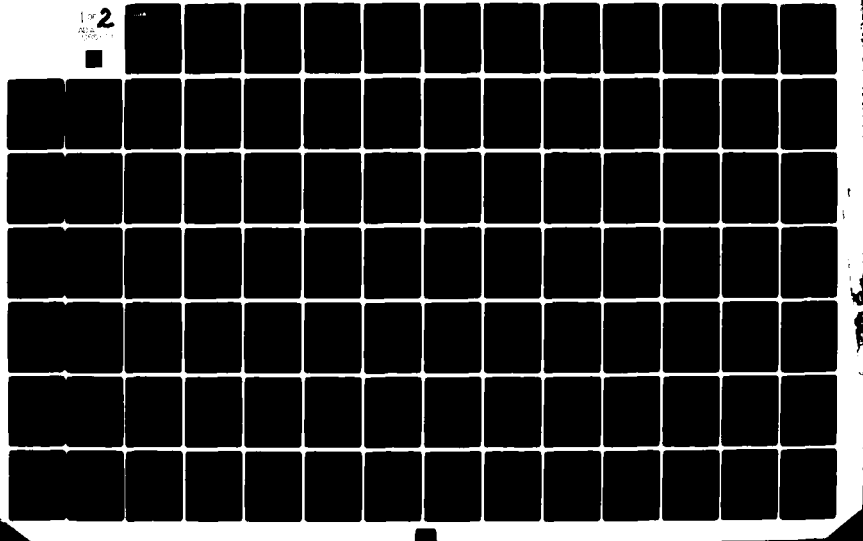


A
8517

LJI-R-80-060

LaJolla INSTITUTE

P.O. BOX 1434 • LA JOLLA • CALIFORNIA 92038 • PHONE (714) 454-8126

DEMOGRAPHICS AND CASUALTY PREDICTION/ANALYSIS

BY: JOHN J. SHEA

FINAL REPORT

CONTRACT NO. DCPA01-79-C-0244

(WORK UNIT NO. 4111C)

FEBRUARY 1980

PREPARED FOR:

FEDERAL EMERGENCY MANAGEMENT AGENCY
OFFICE OF MITIGATION AND RESEARCH
ATTN; MR. JAMES JACOBS, COTR
WASHINGTON, D. C. 20472

PREPARED BY:

LA JOLLA INSTITUTE
1500 WILSON BOULEVARD
ARLINGTON, VA 22209
TELEPHONE: (703) 522-0225

LJI-R-80-060

DEMOGRAPHICS AND CASUALTY PREDICTION/ANALYSIS

By

John J. Shea

FINAL REPORT

Contract No. DCPA01-79-C-0244
(Work Unit 4111C)

February 1980

This report has been reviewed in the Federal Emergency Management Agency and approved for publication. Approval does not signify that the contents necessarily reflect the views and policies of the Federal Emergency Management Agency.

PREPARED FOR:

FEDERAL EMERGENCY MANAGEMENT AGENCY
Office of Mitigation and Research
Attention: Mr. James Jacobs, COTR
Washington, D. C. 20472

PREPARED BY:

LA JOLLA INSTITUTE
1500 Wilson Boulevard
Arlington, VA 22209
Telephone: (703) 522-0225

UNCLASSIFIED

SECURITY CLASSIFICATION OF THIS PAGE (When Data Entered)

REPORT DOCUMENTATION PAGE

READ INSTRUCTIONS BEFORE COMPLETING FORM

1. REPORT NUMBER	2. GOVT ACCESSION NO. AD-A085 170 / 3. RECIPIENT'S CATALOG NUMBER (9)
4. TITLE (and Subtitle) (6) DEMOGRAPHICS AND CASUALTY PREDICTION/ANALYSIS,	5. TYPE OF REPORT & PERIOD COVERED Final Report Jul 1979 — Feb 1980,
	6. PERFORMING ORG. REPORT NUMBER (14) LJI-R-80-060
7. AUTHOR(s) (10) John J. Shea	8. CONTRACT OR GRANT NUMBER(s) (15) DCPA01-79-C-0244
9. PERFORMING ORGANIZATION NAME AND ADDRESS La Jolla Institute P. O. Box 1434 La Jolla, CA 92038	10. PROGRAM ELEMENT, PROJECT, TASK AREA & WORK UNIT NUMBERS Work Unit No. 4111C
11. CONTROLLING OFFICE NAME AND ADDRESS Federal Emergency Management Office of Mitigation and Research Washington, D. C. 20472 (11)	12. REPORT DATE Feb 1980 / 13. NUMBER OF PAGES 116
14. MONITORING AGENCY NAME & ADDRESS (if different from Controlling Office) (12) (12)	15. SECURITY CLASS. (of this report) UNCLASSIFIED / 15a. DECLASSIFICATION DOWNGRADING SCHEDULE

16. DISTRIBUTION STATEMENT (of this Report)

Approved for public release; distribution unlimited.

17. DISTRIBUTION STATEMENT (of the abstract entered in Block 20, if different from Report)

18. SUPPLEMENTARY NOTES

19. KEY WORDS (Continue on reverse side if necessary and identify by block number)

Damage Prediction, Casualty Prediction, Prompt Nuclear Effects, Delayed Nuclear Effects, Air Blast, Fallout, Demographics, Damage Probability, Delivery Accuracy, Dispersion, Blast Hardness, Radiation Shielding, Convex Functions, Bounds, Relocation

20. ABSTRACT (Continue on reverse side if necessary and identify by block number)

This report presents a general method of predicting and bounding casualties from both prompt and delayed effects produced by attacks against population. The method contains analytic sub-models for distributions of population and hardness and for nuclear weapons phenomenology. Relocation schemes which evacuate people to locations where at least some people already reside are characterized abstractly and analyzed parametrically. The general analytic results predict the dispersion/hardness needed to achieve any specified

DD FORM 1 JAN 73 1473

UNCLASSIFIED 393490

SECURITY CLASSIFICATION OF THIS PAGE (When Data Entered)

ABSTRACT (Continued)

outcome against any specified attack size and are used to explore the relative influence of the ingredients of a passive defense system.

ABSTRACT

This report presents a general method for predicting and bounding casualties from both prompt and delayed effects produced by attacks against population. The method contains analytic sub-models for distributions of population and hardness and for nuclear weapons phenomenology. Relocation schemes which evacuate people to locations where at least some people already reside are characterized abstractly and analyzed parametrically. The general analytic results predict the dispersion/hardness needed to achieve any specified outcome against any specified attack size and are used to explore the relative influence of the ingredients of a passive defense system.

FOREWORD

This report completes the presentation of results obtained by La Jolla Institute under Contract No. DCPA01-79-C-0244. Mr. James Jacobs was the FEMA technical monitor.

TABLE OF CONTENTS

LIST OF FIGURES

LIST OF FIGURES, continued

LIST OF TABLES

LIST OF TABLES, continued

SUMMARY

This report presents a general method for predicting and bounding casualties from both prompt and delayed effects produced by nuclear attacks against population. We summarize the major findings and recommendations as follows:

1. The feasibility of interrelating analytically the major ingredients of damage/casualty prediction has been demonstrated by deriving tractable, explicit analytic representations of the interplay among the characteristics of the attack, targets, environment and outcome.

2. Our approach for determining the effective blast protection of a population with mixed, non-uniform protection produces stable, consistent values of protection hardness and accurate estimates of casualties.

3. Relocation schemes which evacuate a region's population to locations where at least some people already reside have been characterized abstractly and analyzed parametrically; in particular, the conditions for, and consequences of, self-contained regional relocation have been determined.

4. It is highly unlikely that any realistic approach could relocate the bulk of the nation's population at population density less than 1,000 to 1,500 people/mi^2, i.e., some 2 to 3 times the population density corresponding to spreading the entire population uniformly over the entire populated area.

5. To achieve moderate survivor fractions for attacks against population with several thousand blast-equivalent megatons, significant blast

hardening is required, even with the most defense-optimistic assumptions about relocation.

6. For attacks against population, the influence of delayed-effects hardness is generally weak, compared to the influence of prompt-effects hardness and dispersion.

7. In view of the results and conclusions presented above, we recommend that

a) the demographics of residential population be analyzed to explore the validity of the apparent universality of normalized rank-ordered population distribution for different geographic regions and to provide a basis for interpreting the rank-ordered population distribution in other commonly used formats (e.g., in terms of political subdivisions)

b) the general analytic approach and results be extended, refined, and applied, e.g., by considering attacks more general than attacks against population, tighter bounds on combined-effects casualties, and specific candidate relocation schemes.

1. INTRODUCTION

This report completes the presentation of results obtained by La Jolla Institute in a continuing investigation supported by Contracts No. DCPA01-78-C-0183 and DCPA01-79-C-0244. Earlier results are presented elsewhere [Ref. 1] and are summarized below as needed. The overriding objective of this effort has been to interrelate analytically the major ingredients of damage/casualty prediction by deriving tractable, explicit analytic expressions of the interplay among the characteristics of the attack, targets, environment and outcome.

In working toward this objective, we have put special emphasis upon nuclear attacks against population and upon the civil defense measures of relocation and hardening. The spirit of the investigation has been to seek not specific numerical results but rather tractable analytic expressions and thereby to understand parametric trends and to explore the meaningfulness, accuracy, and sensitivity of the results. We have accordingly sought solutions for not only the direct problem (i.e., predicting the outcome as a function of the parameters characterizing the target, attack, and environment) but also for the inverse problem of expressing any ingredient of the problem as a function of the others. In particular, we have sought results which prescribe the hardening/dispersion combinations sufficient to guarantee a specified outcome. Such results clearly provide a rational basis for designing passive defense measures and for balancing hardness and dispersion measures.

In Section 2 below, we begin by summarizing our general analytic results (including solutions of the direct and inverse problems discussed above) and their conceptual foundations. We then discuss a major element of each of the two generic civil defense techniques of hardening and dispersion; specifically, we present results for characterizing effective blast hardness and relocation schemes which evacuate people to locations where at least some people already reside. In closing Section 2, we illustrate the application of our general analytic results by presenting a number of specific examples for prompt and delayed casualties and for in-place and relocated populations. In Section 3, we draw conclusions and make recommendations.

2. STRUCTURE OF THE DAMAGE/CASUALTY PREDICTION PROBLEM

In this section, we summarize and illustrate our results concerning the structure of the damage/casualty prediction problem.

2.1 Summary of Analytic Results

Unless otherwise noted, the results presented in this subsection are derived in Ref. 1, frequently in considerably greater generality than indicated below; for complete derivations of the results (including the range of their validity), this reference should be consulted. We begin by recapitulating the ingredients of the problem.

For an attack against population, the target is characterized by its joint population/hardness distribution. The hardness is specified by four parameters: the prompt-effects hardness by a single effective damage overpressure, $\Delta p_{s,50}$; the delayed-effects (i.e., fallout) hardness by the effective protection factor $\langle \rho \rangle$ (i.e., the attenuation of the free-field dose by an individual's surroundings) and by the mean, $D_{eff,m}$, and standard deviation, σ_D, defining the "universal" Gaussian distribution of damage probability vs. total equivalent biological dose to which an individual is exposed. (It will be recalled that the pair $[D_{eff,m}, \sigma_D]$ is customarily taken to be [450R, 75R] and [250R, 50R] for fatalities and casualties, respectively.) The spatial distribution of population is specified by the distribution, F, of cumulative population, Ω, versus cumulative area, A, obtained by successively subdividing the target region into rectangular cells, noting the population

and area of each cell, rank-ordering the cells by population density (i.e., by population divided by area), and summing over the rank-ordered cells. Thus the population distribution (normalized by the total regional population, Ω_{tot}) is given by

$$\frac{\Omega}{\Omega_{tot}} = F\left(\frac{A}{A^*}\right) \tag{1}$$

where A* is a suitable normalizing area. The population density, ω, is given by

$$\omega = \frac{d\Omega}{dA} = \frac{\Omega_{tot}}{A^*} F'\left(\frac{A}{A^*}\right) \tag{2}$$

From the construction of F, it is clear that the population density (and hence F') is positive and decreasing, so that the distribution F is convex. In sum, then, the target is characterized by the four parameters specifing the hardness, plus the two parameters Ω_{tot} and A* which, along with any parameters characterizing the dimensionless distribution F, specify the spatial distribution of the population.

An attack against population targets the first weapon against the most populous cell and sequentially targets cells rank-ordered by population density. To characterize an attack against population, it is clearly necessary to specify the total number, N, and the burst height of the attacking weapons and to specify the yield, Y, and fission fraction, F/Y, of the individual weapons. (To avoid confusion with the symbol introduced in Equation 1 to describe the normalized population distribution, we refer to the fission-yield exclusively

in the fission-fraction combination F/Y.) Since the effective damage overpressure is typically less than 10 psi and never exceeds tens of psi, it suffices to consider two burst-heights: an airburst optimized for the damage overpressure maximizes the prompt-effects damage but produces no fallout and hence no delayed-effects damage; a surface burst maximizes the delayed-effects damage and produces the same prompt-effects damage as any fallout-producing detonation. Therefore, to complete the attack characterization, it suffices to specify either the number, N_S, of surface bursts or the number, N_A, of optimized airbursts, since

$$N = N_A + N_S \tag{3}$$

In sum, then, the attack is characterized by four parameters: Y, F/Y, N, N_S.

The environment for prompt-effects damage is characterized by the ambient pressure, p_o, while the environment for delayed-effects damage is characterized by the "effective fallout" wind, $\underline{W}$, and cross-wind shear, S_c, where, here and throughout this report, a symbol with underscore "_" denotes a vector quantity, while the same symbol without the underscore denotes the magnitude of the vector. In our approach, by suitably formulating fallout phenomenology and employing bounding arguments, we are able to finesse the effects of $\underline{W}$ and S_c, and to obtain delayed-effects damage results independent of these parameters.

The outcome of the attack is characterized by the number of fatalities, Ω_{fat}, or casualties, Ω_{cas}. In stating results, additional affixes have the

obvious interpretations: e.g., $\Omega_{fat,prompt}$ denotes the fatalities from prompt effects while $\Omega_{fat,comb}$ denotes the fatalities from combined (i.e., prompt plus delayed) effects. The outcome may equivalently be expressed in terms of the survivor fraction ε given by

$$\varepsilon = 1 - \frac{\Omega_{fat}}{\Omega_{tot}} \tag{4}$$

The parameters introduced above characterize the ingredients of the damage/casualty prediction problem. For attacks against population by contemporary nuclear weapon delivery systems, we find that these ingredients are interrelated via

$$\frac{\Omega_{fat,prompt}}{\Omega_{tot}} = F\left(\frac{\tau N}{A^*}\left[\nu_s\, s_{50,S}^2 + (1-\nu_s) s_{50,A}^2\right]\right) \leq F\left(\frac{\tau N s_{50,A}^2}{A^*}\right) \tag{5}$$

$$\frac{\Omega_{fat,comb}}{\Omega_{tot}} \leq F\left(\frac{\tau N s_{50,A}^2}{A^*}\left[1+\hat{\phi}\right]\right) \tag{6}$$

where

$$\tau = \left\{\begin{matrix} 2 \\ \pi \end{matrix}\right\} \quad \text{for} \quad \left\{\begin{matrix} \text{offense} \\ \text{defense} \end{matrix}\right\} \text{ - conservative, i.e., } \left\{\begin{matrix} \text{lower} \\ \text{upper} \end{matrix}\right\} \text{ bounds on fatalities} \tag{7}$$

$$\nu_S = N_S/N \tag{8}$$

$$s_{50,A} = \hat{\eta}_A \, (Y/p_o)^{1/3} \left(\frac{\Delta p_{s,50}}{p_o} \right)^{-3/5} \qquad \hat{\eta}_A = 1.022 \tag{9}$$

$$s_{50,S} = \hat{\eta}_S \, (Y/p_o)^{1/3} \left[-1 + \left\langle 1+3.18 \, \frac{\Delta p_{s,50}}{p_o} \right\rangle^{1/2} \right]^{-2/3} \qquad \hat{\eta}_S = 0.776 \tag{10}$$

$$\hat{\phi} = \frac{\nu_S}{\hat{\kappa}} \left[\frac{\hat{\psi}^*}{\langle \rho \rangle / (F/Y)} - 1 \right] \tag{11}$$

$$\hat{\kappa} = \frac{s_{50,A}^2}{s_{50,A}^2 - s_{50,S}^2} \tag{12}$$

$$\hat{\psi}^* = \frac{\Psi_{max} \Lambda_o / D_{eff}^*}{\tau (s_{50,A}^2 - s_{50,S}^2)} \tag{13}$$

$$\Psi_{max} = 0.4869 \tag{14}$$

$$\Lambda_o = \left[\frac{1.0015 \times 10^6 Y}{(1+0.2213 \log_{10} Y)^{0.382}} \right] \text{R-mi}^2 \qquad Y \text{ in Mt} \tag{15}$$

$$D_{eff}^* = D_{eff,m} \left[1 - \left(\frac{\sigma_D}{D_{eff,m}} \right)^2 \right] \tag{16}$$

The parameters $s_{50,A}$ and $s_{50,S}$ express the distance to which the damage overpressure $\Delta p_{s,50}$ extends for an optimized airburst and for a surface burst, respectively. The parameters Ψ_{max} and Λ_o arise from our formulation of fallout phenomenology and, in particular, from our result that, for a single detonation, the isodose area (i.e., the area within an isodose contour, or, equivalently, the area within which a given dose is exceeded) corresponding to a free-field dose D is given by

$$A_{isodose} = A\Phi\left(\frac{AD}{\Lambda}\right) = \frac{\Lambda}{D}\Psi\left(\frac{AD}{\Lambda}\right) \tag{17}$$

where

$$\Lambda = \Lambda_o(F/Y) \tag{18}$$

and the normalizing area A is given by

$$A = \sigma_H S_c W T^2 \tag{19}$$

and the parameters σ_H and T depend on yield only and can be well approximated [Ref. 2] for yields in the megaton range as

$$\sigma_H = [7.5 + 1.5 \log_{10} Y]\text{kft} \qquad Y \text{ in Mt} \tag{20}$$

$$T = [7.5 + 1.66 \log_{10} Y]\text{hr} \qquad Y \text{ in Mt} \tag{21}$$

and the functions Φ and Ψ are shown in Figure 1. As may be seen from Figure 1, the parameter of Equation 14 is indeed the maximum value of the function Ψ, i.e.,

$$\Psi_{max} = 0.4869 = \Psi(w=w^*=0.6834) \qquad (22)$$

By selecting aim-points at (or above) the center of the N most densely populated cells, an attack with N weapons is guaranteed to achieve the prompt-effects fatalities given by Equation 5, with $\tau=2$. Conversely, an attack with N weapons cannot achieve greater prompt-effects fatalities than those given by Equation 5, with $\tau=\pi$. Therefore, the actual number of prompt-effects fatalities is given by Equation 5 for some value of τ between 2 and π; moreover, the values of 2 and π for τ provide the bounds indicated by Equation 7. It is clear that an attack employing airbursts exclusively (i.e., $\nu_s=0$) is feasible and maximizes the prompt-effects fatalities. The upper-bound on combined fatalities as expressed by Equation 6 is derived by upper bounding the size and population of the fallout region; although lower bounds or alternative upper bounds could also be derived, the result expressed by Equation 6 is especially powerful, as we describe below; here, and throughout this report, we follow the convention that "Equation _" is a name for a mathematical relationship which may, but need not be, an equality.

It is clear that by presenting the outcome as an explicit analytic function of the problem's other ingredients, Equations 5 and 6 solve the "direct" problem discussed above. Moreover, the solution of the inverse problem is readily inferred. Specifically, Equation 5 immediately implies the equivalent

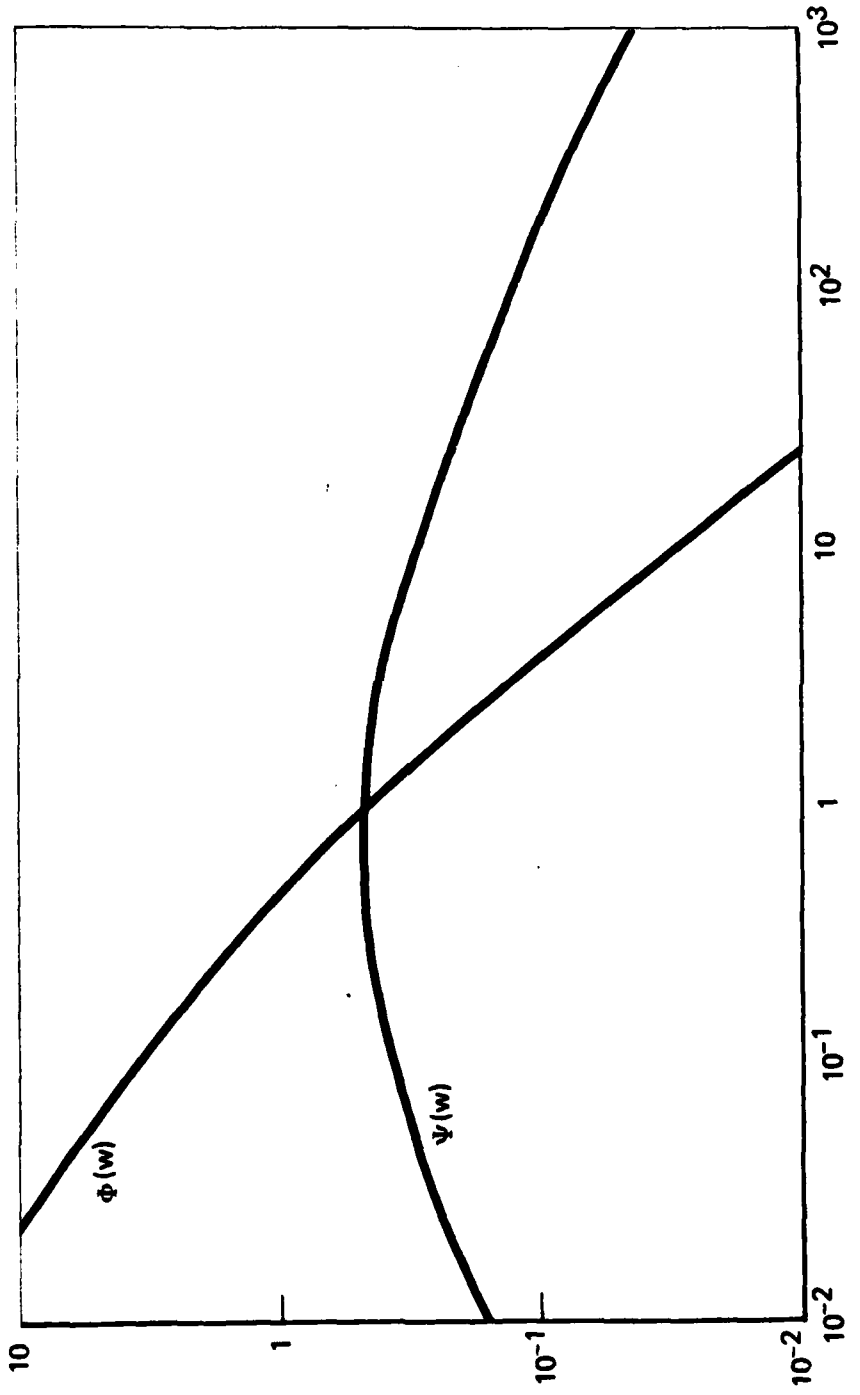

Figure 1. The Functions $\Phi(w)$ and $\Psi(w)$ vs. w

blast yield $NY^{2/3}$ (popularly described as "equivalent megatons") needed to achieve a specific outcome against a specific target. Likewise, the combination of dispersion and prompt-effects hardness to achieve a specified outcome is given by

$$\left(\frac{\Delta p_{s,50}}{p_o}\right)^{6/5} A_{cum}(1-\varepsilon) = \tau N \langle \hat{n}_A (Y/p_o)^{1/3} \rangle^2 \qquad (23)$$

where

$$A_{cum}(z) = A^* F^{-1}(z) = \text{most densely populated area containing fraction z of total population, } 0 \leq z \leq 1 \qquad (24)$$

Clearly any joint hardness/dispersion distribution satisfying Equation 23 guarantees the specified outcome (i.e., prompt-effects survivors) against the specified attack. If either the hardness or the spatial distribution of the population is specified independently, then the other parameter is readily inferred from Equation 23.

From Equation 6, it is clear that the combined (prompt plus delayed) fatalities from a mixed surface/airburst attack cannot exceed the combined (exclusively prompt) fatalities from a pure airburst attack if $\hat{\phi}$ is negative; from Equations 11 and 13, the condition that $\hat{\phi}$ be negative is equivalent to the condition

$$\frac{\langle\rho\rangle}{F/Y} > \hat{\psi} = \frac{\psi_{max}\Lambda_o/D^*_{eff}}{\tau(s^2_{50,A} - s^2_{50,S})} \qquad (25)$$

From Equations 9, 10 and 15 (and the fact that the denominator in Equation 15 exhibits negligible variation with yield), it is clear that the parameter $\hat{\psi}^*$ depends only on $\Delta p_{s,50}$ and Y with the yield dependence given by

$$\hat{\psi}^* \sim Y^{1/3} \qquad (26)$$

Since the yield of contemporary strategic weapons lies within a factor of 3^3 about one megaton (i.e., between 37 kt and 27 Mt), $\hat{\psi}^*$ varies with yield by at most a factor of 3. Moreover, for attacks which produce the same prompt-effects damage and which therefore have the same blast-equivalent yield $NY^{2/3}$, it follows from Equation 26 that

$$\hat{\psi}^* \sim N^{-1/2} \quad \text{for constant } NY^{2/3} \qquad (27)$$

The significance of Equations 6 and 25 lies in the fact that radiation shielding sufficient to satisfy Equation 25 accomplishes as much as any amount of shielding can accomplish--in the sense that any additional shielding can be obviated by the offense's simply raising the burst height and thereby producing greater casualties. The critical value of shielding (as characterized by the attenuation $\langle\rho\rangle$ or protection factor PF) depends only on yield (as $Y^{1/3}$)

and on the damage overpressure and is completely independent of all the other variable ingredients of the problem--independent of how the population is distributed in an absolute sense, independent of how the population is distributed in a rank-ordered sense, independent of the size of the attack, independent of where the detonations occur, independent of what the winds and weather are, independent of what the number of fatalities is.

An approach to selecting performance criteria for passive defense emerges naturally from the results presented above: first the dispersion and prompt-effects hardness are prescribed by Equation 23, then the delayed-effects hardness (corresponding to the prescribed prompt-effects hardness) is given by Equation 25. In this approach, the required dispersion and prompt-effects hardness depend upon the desired outcome and upon the size of the attack, while the delayed-effects hardness depends significantly upon only the prompt-effects hardness. Delayed-effects hardness better than that prescribed by Equation 25 may reduce casualties from some attacks, but obviously cannot possibly reduce casualties from the pure-airburst attack. Moreover, if the delayed-effects hardness satisfies Equation 25, then even if the attack size increases beyond the design level, it remains true that no attack can produce more casualties from combined effects than those produced by prompt-effects from a pure airburst attack--even though the latter casualties increase.

In the results presented above, the target hardness which can be modified by civil defense efforts is represented by two parameters: $\Delta p_{s,50}$ and $\langle \rho \rangle$. In reality, the protection of the entire population does not possess a single homogeneous hardness for prompt or delayed effects, but can be decomposed into a

finite number of (mutually exclusive and cumulatively exhaustive) classes of homogeneous hardness. Given the latter more realistic and fine-grained distribution of hardness, it is possible (as shown in Ref. 1) to define an equivalent uniform hardness so that Equations 5 and 6 and their implications remain valid. For example, if there are M exposure environments for delayed effects, with each individual such environment characterized by the protection factor ρ_j and containing the fraction β_j of the total population, then

$$\frac{1}{\langle\rho\rangle} = \sum_{j=1}^{M} \frac{\beta_j}{\rho_j} \tag{28}$$

Similarly, if each exposure environment for prompt effects contains fraction α_j of the total population and is characterized by the damage overpressure $\Delta p_{s,50,j}$, then an analogous (but slightly more complicated) expression gives the equivalent uniform hardness $\Delta p_{s,50}$ in terms of all the α_j and $\Delta p_{s,50,j}$; we discuss and illustrate this expression in Section 2.2 below.

Dispersion, the other target property which appears in the results presented above and which can be modified by civil defense efforts, is represented by the rank-ordered distribution F and its inverse. It is clear that any physically realizable spatial distribution of population determines a unique rank-ordered F; the same rank-ordered F could (in principle, if not in practice) arise from different spatial distributions of population. The

distribution of residential (i.e., "in-place") population is the single most important distribution, both for its own sake and as a starting-point for relocated distributions. By analyzing the residential population of the entire nation and of three sub-regions (consisting of a 12-state Northeastern complex, a 4-state Midwestern complex, and the single state of California, respectively), we find [Ref. 1] that the residential population of each of these regions determines a rank-ordered distribution which is well represented by $F=F_0$ where

$$F_0(w) = 1-e^{-w^{\lambda}} \qquad \lambda = 0.63 \tag{29}$$

The Northeastern complex consists of Connecticut, Delaware, District of Columbia, Maine, Maryland, Massachusetts, New Hampshire, New Jersey, New York, Pennsylvania, Rhode Island, and Vermont; the Midwestern region consists of Illinois, Indiana, Michigan and Ohio. Moreover, we find that the total populated area of each region is well approximated as $10A^*$. Consequently, different regions share the same normalized rank-ordered distribution of residential population and differ only in the amount of unpopulated area and, of course, in the absolute scale of the distribution as reflected in Ω_{tot} and A^*. In Section 2.3 below, we analyze the implications of these results for relocation schemes which evacuate people to locations where at least some people already reside.

While the preceding summary of analytic results is a complete statement of the results quoted and occasionally suggests the derivation thereof, a more coherent presentation of their derivation may be desired. To this end, we now present an overview (adapted from Ref. 1) of their conceptual foundation. For additional details, the reader should consult the complete reference

which provides a precise statement of the damage/casualty prediction problem for arbitrary targeting by the attacker and, for attacks against population, presents a general method for predicting and bounding casualties from both prompt and delayed effects.

A precise and rigorous statement of the damage/casualty prediction problem results from adopting the conceptual framework wherein targets are susceptible in a finite number of damage levels to a finite number of different "loading" types and are found in a finite number of mutually exclusive exposure environments, with each exposure environment characterized, for each damage level, by its susceptibility to each of the loadings. A specific damage/casualty prediction technique is essentially defined by its treatment of eight critical characteristics. We illustrate this viewpoint by describing in explicit detail how each of these eight characteristics is treated in four specific techniques which are in current use and which collectively span the range of diversity, complexity, and detail to be found in contemporary approaches.

To introduce the elements of the original approach presented here and to lay the foundation for the general method developed here, we organize the discussion around the eight critical characteristics discussed above. These methodological auxiliaries to the major results show that

a) a step-function ("cookie-cutter") is a valid representation of prompt-effects damage probability; this result is derived by theoretical arguments and verified by comparison with detailed numerical results

b) damage degradation due to delivery system inaccuracy is negligible for the range of targets and attacks considered here; this result

emerges, in the limit, from a general analysis which demonstrates that probability of damage to point and area targets depends on at most two overpressures (characterizing the offense and defense, respectively) and is tightly bounded by prescribing merely the ratio of these two characteristic overpressures

c) the probabilistic nature of casualty prediction does not introduce significant uncertainty into the predictions

d) for fallout-producing detonations, the magnitude and location of the maximum dose and the variation thereof with wind can be expressed in tractable analytic terms, valid for all physically realistic winds; these results are derived from the general WSEG-10 fallout phenomenology

e) the area within isodose contours from fallout-producing detonations can be expressed in simple analytic terms and upper-bounded independently of wind structure; this result follows from reformulating WSEG-10 fallout phenomenology in a dimensionless form which provides "universal" isodose contours

f) the normalized distribution of residential population (rank-ordered by population density) versus cumulative area occupied by that population is essentially the same for the regions analyzed (i.e., the continental United States, a 12-state Northeastern region, a 4-four state Midwestern region, California) and is described by a simple analytic expression; preliminary results indicate that in all regions, the entire populated area is approximately twenty times the area containing the most densley populated half of the total

population and, consequently, that regions differ in the amount of unpopulated area which they contain, but do not differ in the way in which populated area is filled.

Because different geographic regions appear to share the same normalized rank-ordered distribution of residential population, relocation strategies which evacuate people to locations where at least some people already reside are more nearly similar than dissimilar for different regions; considerations of relocation on a national scale may require that different parametric ranges of the common normalized distribution be emphasized in different geographic regions.

The application of our general approach for predicting prompt-effects casualties to 40 specific families of attacks (corresponding to every combination of four geographic regions, two burst-heights, and five aim-point spacings) against residential population has

a) produced numerical results wherein the joint population/hardness distribution is represented with the most fine-grained detail available and with the greatest defense optimism (i.e., "best available shelter")

b) corroborated analytic simplifications in the general approach whereby arbitrary joint population/hardness distributions are successively reduced to the more tractable distributions of multiple-uniform-hardness and of single effective uniform hardness

Our general analytic results predict

a) significant dispersion/hardness are needed to achieve moderate levels of prompt-effects survivors from attacks against population by a few thousands of megaton-size weapons

b) modest amounts of radiation shielding suffice to guarantee that no attack against population can produce more casualties by blast and fallout combined than the casualties produced by blast alone from the same number of optimized airbursts--regardless of the spatial distribution of the population, regardless of the size and location of the attack, regardless of the wind and weather, regardless of the number of casualties

c) both accurate numerical values and generalized scaling laws to understand trends, sensitivites, regularities.

Having indicated the origin of the analytic results presented above, we now turn to extending and applying these results.

2.2 Effective Prompt-Effects Hardness

We now consider the realistic situation wherein there are M (mutually exclusive and collectively exhaustive) exposure environments for prompt effects, with each such environment characterized by its damage overpressure, $\Delta p_{s,50,j}$, and containing the fraction α_j of the total population, $1 \leq j \leq M$; we take the exposure environments to be ordered in terms of increasing damage overpressure so that exposure environments 1 and M are the "softest" and "hardest", respectively. The damage distance $s_{50,j}$ is related to the damage overpressure $\Delta p_{s,50,j}$ via Equations 9 and 10 for optimized airbursts and surface bursts,

respectively. Since our intent is to explore the notion of effective blast hardness, we restrict attention in this subsection to prompt-effects casualties.

By rank-ordering cells of characteristic (center-to-corner) size $\hat{s}$ and selecting aim-points at or above the centers of the N most densely populated cells, an attack with N weapons produces prompt-effects fatalities given by

$$V(\hat{s}) = \langle Q \rangle F\left(\frac{\tau N \hat{s}^2}{A^*}\right) = \left[\sum_{j=1}^{M} \alpha_j Q\left(\frac{s_{50,j}}{\hat{s}}\right)\right] F\left(\frac{\tau N \hat{s}^2}{A^*}\right) \tag{30}$$

where the population-weighted coverage coefficient $\langle Q \rangle$ is given the obvious definition in terms of the coverage coefficient Q given by

$$Q(w) = \begin{cases} (\pi/2)\ w^2 & 0 \le w \le 2^{-1/2} \\ w^2\ [u + \arccos u] & 2^{-1/2} \le w \le 1 \\ 1 & 1 \le w < \infty \end{cases} \tag{31}$$

$$u = \frac{1}{w}\left(2 - \frac{1}{w^2}\right)^{1/2} \tag{32}$$

It is clear that Q(w) is an increasing function of w and consequently that $\langle Q \rangle$ in Equation 30 is a decreasing function of $\hat{s}$; F in (3) is, of course, an increasing function of $\hat{s}$. Considered as a function of $\hat{s}$, $V(\hat{s})$ has (as shown

in Ref. 1) for $\hat{s}$ between $s_{50,M}$ and $2^{1/2}s_{50,1}$ a unique global maximum at, say, $\hat{s}^*$. The effective damage distance and damage overpressure are given by

$$s_{50} = \hat{s}^* \, Q^{-1}\left(\sum_{j=1}^{M} \alpha_j \, Q\left(\frac{s_{50,j}}{\hat{s}^*}\right)\right) \tag{33}$$

$$\Delta p_{s,50} = \Delta p_s(s_{50}) \tag{34}$$

In terms of these effective values, we take the prompt-effects fatalities to be given (as in Equation 5 above) by

$$\frac{\Omega_{fat}}{\Omega_{tot}} = F\left(\frac{\tau N s_{50}^{\,2}}{A^*}\right) \tag{35}$$

In general, the effective hardness defined by Equations 33 and 34 depends on N and F. We show below that this dependence is weak. Moreover, we show that Equation 35 underestimates the "exact" maximum $V(\hat{s}=\hat{s}^*)$ by a negligibly small amount and therefore that the combination of Equations 33, 34 and 35 provides a valid representation of effective hardness and casualties for a non-uniform population.

Before investigating more complicated situations, we discuss the simplest case, where M = 1, i.e., there is but a single uniform hardness. It is clear from Equations 33 and 34 that our general approach specializes

correctly in this case to the given single hardness. Nevertheless it is instructive to explore the variation of $\hat{s}^*$ and $V(\hat{s}^*)$. For concreteness (and without any real loss of generality), in this and all other cases discussed in this subsection, we restrict attention to surface bursts and to the distribution $F=F_o$ which is given by Equation 29 and which accurately represents American residential population. Our results are summarized in Tables 1 and 2 and plotted in Figures 2 and 3. We see that as $\tau N s_{50}^2/A^*$ increases, $\hat{s}^*/s_{50}$ decreases steadily from 1.3502 toward 1 and that the ratio of $V(\hat{s}^*)$ to $F(\tau N s_{50}^2/A^*)$ decreases steadily from 1.2289 toward 1. However, the difference between these two estimates of fatalities rises to a maximum of 0.0487 for $\tau N s_{50}^2/A^* = 0.433$ and then decreases steadily. The "exact" maximum at $\hat{s}^*$ greater than s_{50} corresponds, of course, to targeting for an overpressure somewhat less than $\Delta p_{s,50}$ and accepting a smaller fraction of fatalities per cell in return for targeting cells with a greater total area. The approximation (underestimation of the "exact" maximum) embodied (via Equations 33 and 34) in Equation 35 never significantly underestimates the number of fatalities and may legitimately be interpreted as enlarging the region in parameter-space wherein the approximations underlying Equation 35 are valid.

To illustrate the more general case of multiple exposure environments, we consider three examples wherein the damage overpressures $\Delta p_{s,50,j}$ are the same but the occupancy fractions α_j are different. Specifically, we consider M=4 exposure environments with j = 1,2,3,4 corresponding to damage

Table 1

Location and Magnitude of Exact Maximum of Prompt Fatalities - Single Exposure Environment

$\tau N s_{50}^2/A^*$	$\hat{s}^*/s_{50}$	$s_{50}/\hat{s}^*$	$\langle Q\rangle(\hat{s}=\hat{s}^*)$	$F(\tau N \hat{s}^{*2}/A^*)$	$V(\hat{s}=\hat{s}^*)$
10^{-6}	1.3502	0.7406	0.8418	2.422×10^{-4}	2.039×10^{-4}
10^{-5}	1.3501	0.7407	0.8419	1.033×10^{-3}	8.696×10^{-4}
10^{-4}	1.3497	0.7409	0.8422	4.397×10^{-3}	3.703×10^{-3}
10^{-3}	1.3481	0.7418	0.8435	0.0186	0.0157
10^{-2}	1.3409	0.7458	0.8491	0.0764	0.0649
0.1	1.3093	0.7638	0.8724	0.2805	0.2447
0.2	1.2865	0.7773	0.8881	0.3925	0.3485
0.3	1.2682	0.7885	0.9001	0.4684	0.4216
0.4	1.2526	0.7983	0.9099	0.5256	0.4782
0.5	1.2390	0.8071	0.9182	0.5711	0.5243
0.6	1.2268	0.8152	0.9253	0.6085	0.5630
0.7	1.2158	0.8225	0.9315	0.6400	0.5962
0.8	1.2057	0.8294	0.9369	0.6671	0.6250
0.9	1.1966	0.8357	0.9418	0.6906	0.6504
1.0	1.1881	0.8417	0.9461	0.7114	0.6730
1.5	1.1539	0.8666	0.9623	0.7870	0.7573
2.0	1.1288	0.8859	0.9727	0.8352	0.8124
3.0	1.0942	0.9139	0.9847	0.8933	0.8796
4.0	0.0713	0.9335	0.9909	0.9266	0.9182
5.0	0.0552	0.9477	0.9944	0.9476	0.9423
6.0	1.0434	0.9584	0.9965	0.9617	0.9583
7.0	1.0345	0.9666	0.9977	0.9715	0.9693
8.0	1.0277	0.9730	0.9985	0.9784	0.9770
9.0	1.0224	0.9781	0.9990	0.9835	0.9826
10.0	1.0182	0.9821	0.9994	0.9873	0.9866

Table 2

Comparison of Exact and Approximate Values of Maximum Prompt Fatalities - Single Exposure Environment

$\tau Ns_{50}^2/A^*$	$F(\tau Ns_{50}^2/A^*)$	$V(\hat{s}=\hat{s}^*)$	$\frac{V(\hat{s}=\hat{s}^*)}{F(\tau Ns_{50}^2/A^*)}$	$V(\hat{s}=\hat{s}^*) - F(\tau Ns_{50}^2/A^*$
10^{-6}	1.659×10^{-4}	2.039×10^{-4}	1.2289	3.80×10^{-5}
10^{-5}	7.077×10^{-4}	8.696×10^{-4}	1.2288	2.619×10^{-4}
10^{-4}	3.015×10^{-3}	3.703×10^{-3}	1.2281	6.878×10^{-4}
10^{-3}	0.0128	0.0157	1.2252	0.0029
10^{-2}	0.0535	0.0649	1.2139	0.0114
0.1	0.2090	0.2447	1.1710	0.0357
0.2	0.3043	0.3485	1.1455	0.0443
0.3	0.3740	0.4216	1.1273	0.0476
0.4	0.4296	0.4782	1.1132	0.0486
0.5	0.4760	0.5243	1.1016	0.0484
0.6	0.5156	0.5630	1.0920	0.0474
0.7	0.5501	0.5962	1.0837	0.0460
0.8	0.5806	0.6250	1.0765	0.0444
0.9	0.6077	0.6504	1.0703	0.0427
1.0	0.6321	0.6730	1.0647	0.0409
1.5	0.7250	0.7573	1.0445	0.0323
2.0	0.7872	0.8124	1.0319	0.0251
3.0	0.8644	0.8796	1.0176	0.0152
4.0	0.9088	0.9182	1.0103	0.0094
5.0	0.9365	0.9423	1.0063	0.0059
6.0	0.9546	0.9583	1.0039	0.0037
7.0	0.9669	0.9693	1.0025	0.0024
8.0	0.9754	0.9770	1.0016	0.0016
9.0	0.9815	0.9826	1.0010	0.0010
10.0	0.9860	0.9866	1.0007	0.0007

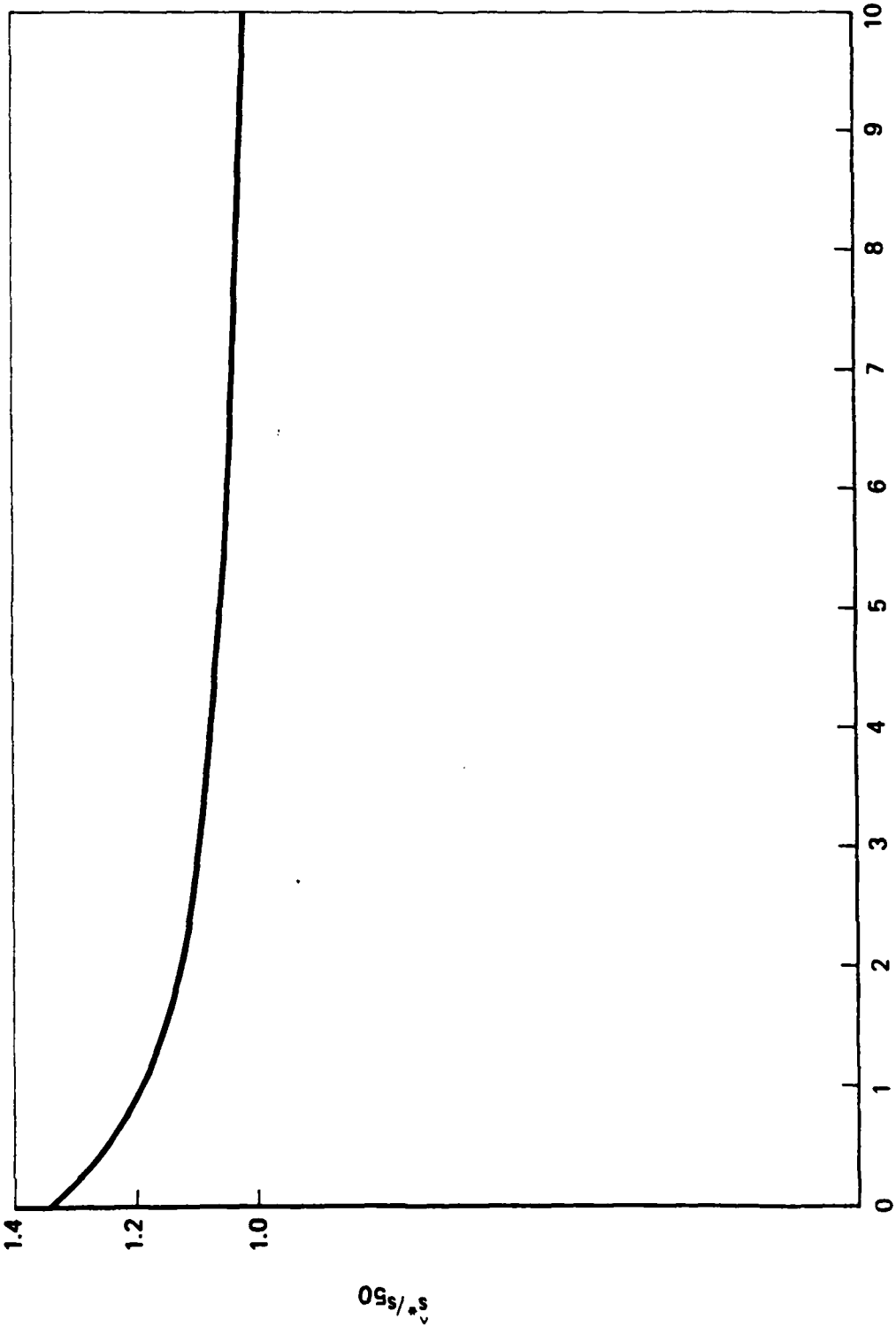

Figure 2. The Parameter $\hat{s}^*/s_{50}$ vs $\tau Ns_{50}^2/A^*$ - Single Exposure Environment

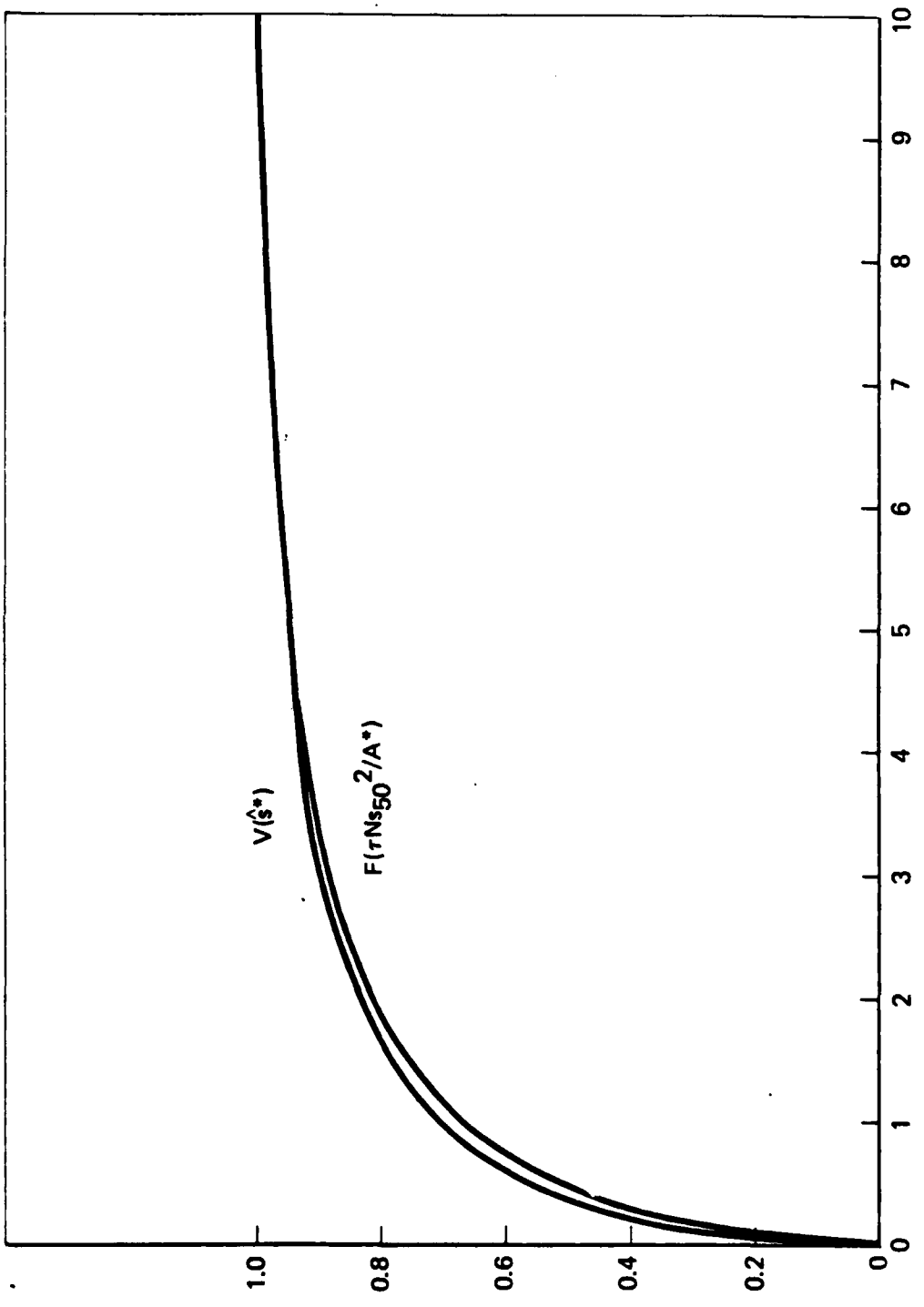

Figure 3. $V(\hat{s}^*)$ and $F(\tau Ns_{50}^2/A^*)$ vs. $\tau Ns_{50}^2/A^*$ - Single Exposure Environment

overpressures of 5, 8, 10 and 35 psi, respectively, and hence to DCPA shelter types G/H/I, E/F, B/C/D, and A, respectively. (For a discussion of DCPA shelter types, cf. Ref. 3.) For the Y = 1 Mt surface bursts considered here, the damage distances $s_{50,j}$ are 2.869, 2.216, 1.969 and 1.076 mi for j = 1,2,3,4 respectively; here, and throughout this report, "mile" denotes a statute mile of 5280 ft = 1.6093 km. The occupancy fractions are selected from the twenty combinations of four regions (Nation, Northeast, Midwest, California) and five cell sizes (length of cell side corresponding to 1, 2, 4, 6, 15 min.) studied earlier (cf. Table 8, Ref. 1). For each of these 20 combinations, the residential population within each cell is located in the best (i.e., highest damage overpressure) shelter available in the cell so that, in each cell, first the 35-psi shelters are filled to capacity, then the 10-psi shelters, etc.; it is assumed that everyone is located in a shelter of at least 5 psi damage overpressure. The three particular sets of occupancy fractions discussed here correspond to (California, 1 min. cell), (Nation, 2 min. cell) and (Northeast, 15 min. cell) and are chosen to represent "soft", "nominal", and "hard" postures, respectively. Although these three examples are not indicative of "softness" or "hardness" in an absolute sense, they are the extremes of the 20 cases studied and doubtless do bracket the hardness of national residential population in "best available shelter". For descriptive simplicity throughout this subsection, we continue to refer to them as "soft", "nominal" and "hard". The numerical characterization of the three examples is given in Table 3. It must be emphasized that the tabulated occupancy fractions serve here to characterize the three postures considered, and are not restricted to specific regions or cell sizes.

Table 3

Characterization of Three Hardness Postures -
Multiple Exposure Environments

j	$\Delta p_{s,50,j}$ psi	$s_{50,j}$ mi.	α_j for		
			Soft Posture	Nominal Posture	Hard Posture
1	5	2.869	0.6884	0.3471	0.0073
2	8	2.216	0.0453	0.0320	0.0073
3	10	1.969	0.2537	0.5984	0.9221
4	35	1.076	0.0126	0.0225	0.0633

For these three examples, we now present numerical results obtained by specializing Equation 30 for τ=2 and Equations 1 and 29 for $A^* = 4 \times 10^4$ mi^2 corresponding, respectively, to offense-conservative results for the entire nation. The behavior of $V(\hat{s})$ as a function of cell size is illustrated in Table 4

Table 4

$V(\hat{s})$ for Nominal Hardness Posture and Several Values of $\hat{s}$ and N

$\hat{s}$,mi.	N = 30	10^2	3×10^2	10^3	3×10^3	10^4
1	0.0159	0.0336	0.0661	0.1358	0.2530	0.4635
1.5	0.0262	0.0552	0.1072	0.2150	0.3833	0.6429
2	0.0372	0.0777	0.1491	0.2913	0.4963	0.7652
2.5	0.0458	0.0949	0.1800	0.3421	0.5570	0.7948
3	0.0485	0.0999	0.1868	0.3454	0.5380	0.7171
3.5	0.0481	0.0984	0.1816	0.3264	0.4871	0.6122
4	0.0461	0.0936	0.1704	0.2979	0.4267	0.5105
4.5	0.0421	0.0847	0.1520	0.2584	0.3562	0.4093
5	0.0386	0.0771	0.1365	0.2258	0.3002	0.3339
5.5	0.0357	0.0707	0.1234	0.1987	0.2555	0.2771
6	0.0332	0.0653	0.1123	0.1760	0.2196	0.2334

and Figure 4 which list and plot, respectively, the magnitude of $V(\hat{s})$ as a function of $\hat{s}$ for the nominal hardness posture and for several values of N. We see that, for each values of N, $V(\hat{s})$ rises to a maximum and then decreases as $\hat{s}$ increases. For each of the three hardness postures and for several values of N, we have determined the location, $\hat{s}^*$, and magnitude, $V(\hat{s}^*)$, of this maximum; the results are displayed in Table 5. Having determined $\hat{s}^*$, we invoke Equation 33 to find s_{50} and $F(\tau N s_{50}^2/A^*)$, with the results shown in Table 6. We note that as the attack size increases, then $\hat{s}^*$ decreases steadily, $s_{50}/\hat{s}^*$ increases (i.e., $\hat{s}^*/s_{50}$ decreases) steadily toward 1, and s_{50} decreases steadily, but relatively slowly; the relative variation in s_{50} is three to five times less than that of $\hat{s}^*$. As N increases, the difference between the "exact" maximum $V(\hat{s}^*)$ and $F(\tau N s_{50}^2/A^*)$ increases to a maximum and then decreases steadily; the maximum value of this difference is relatively small (less than five percent). For the most part, this behavior is precisely that demonstrated earlier for the case of single uniform hardness. These results are depicted in Figures 5, 7, and 9 which present $\hat{s}^*$ and s_{50} versus N for the soft, nominal, and hard postures, respectively, and in Figures 6, 8 and 10 which present $V(\hat{s}^*)$ and $F(\tau N s_{50}^2/A^*)$ in like fashion.

Having determined the damage distance s_{50}, we obtain the corresponding damage overpressure from Equation 34. In Table 7, we summarize the results for s_{50} and $\Delta p_{s,50}$ for all three hardness postures and for several values of N; these results for s_{50} and $\Delta p_{s,50}$ are plotted in Figures 11 and 12, respectively.

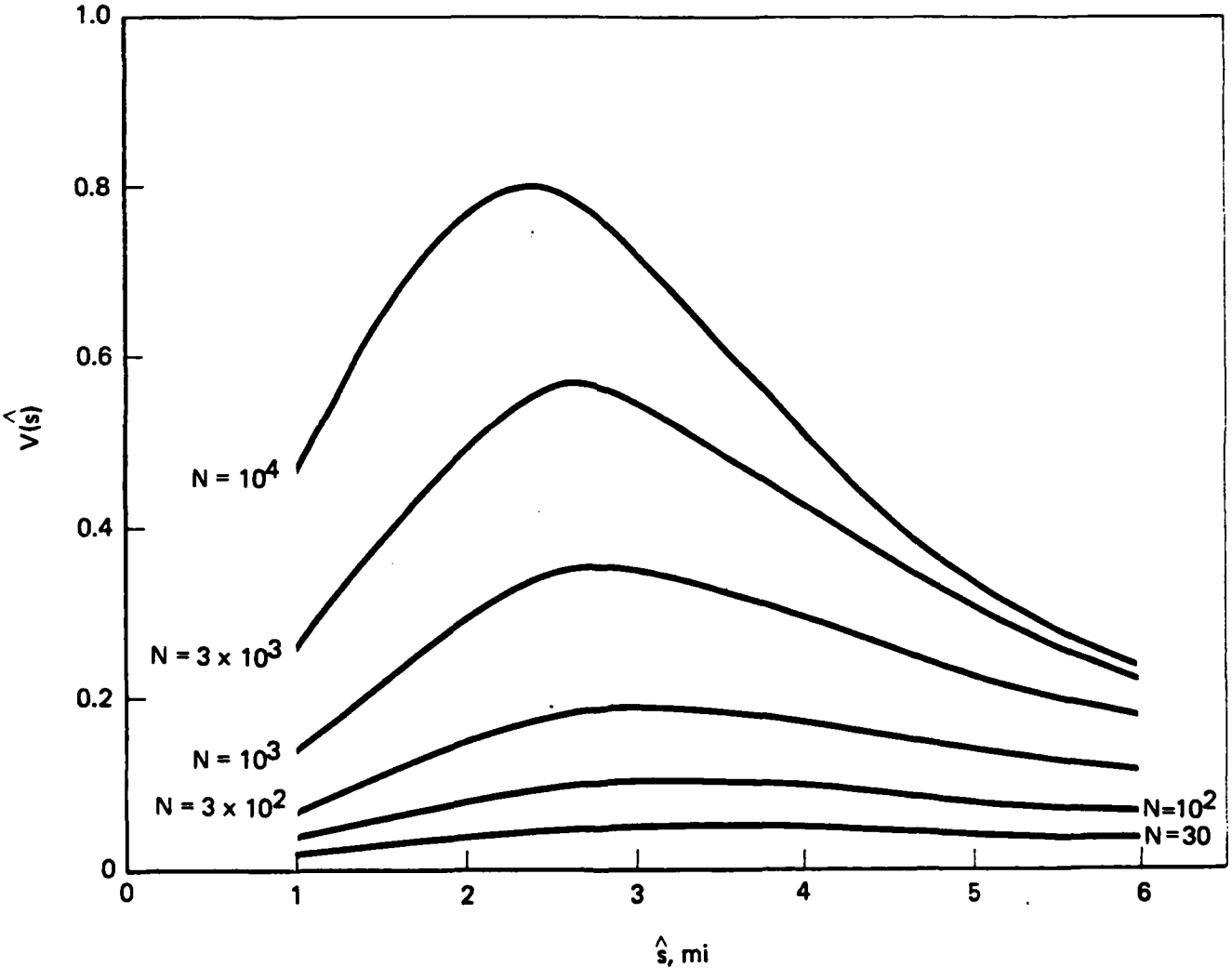

Figure 4. $V(\hat{s})$ vs. $\hat{s}$ for Nominal Posture and Several Values of N

Table 5

Location and Magnitude of $V(\hat{s}^*)$ for Three Hardness Postures

Posture	N	$\hat{s}^*$,mi.	$\langle Q \rangle(\hat{s}=\hat{s}^*)$	$F(\tau N \hat{s}^{*2}/A^*)$	$V(\hat{s}=\hat{s}^*)$
Soft	30	3.731	0.7426	0.0808	0.0600
	10^2	3.679	0.7549	0.1619	0.1222
	$3x10^2$	3.582	0.7777	0.2891	0.2248
	10^3	3.372	0.8244	0.4909	0.4047
	$3x10^3$	3.085	0.8828	0.7006	0.6185
	10^4	2.704	0.9425	0.8870	0.8360
Nominal	30	3.119	0.7469	0.0650	0.0485
	10^2	3.022	0.7757	0.1288	0.0999
	$3x10^2$	2.784	0.8517	0.2200	0.1873
	10^3	2.759	0.8598	0.4080	0.3508
	$3x10^3$	2.648	0.8895	0.6302	0.5606
	10^4	2.375	0.9466	0.8431	0.7981
Hard	30	2.647	0.8114	0.0532	0.0431
	10^2	2.632	0.8170	0.1094	0.0893
	$3x10^2$	2.603	0.8275	0.2040	0.1688
	10^3	2.536	0.8504	0.3760	0.3197
	$3x10^3$	2.419	0.8866	0.5883	0.5216
	10^4	2.222	0.9351	0.8178	0.7647

Table 6

Effective Damage Distance and Casualties for Three Hardness Postures

Posture	N	$\hat{s}^*$,mi.	$s_{50}/\hat{s}^*$	s_{50},mi.	$F(\tau N s_{50}^2/A^*)$
Soft	30	3.731	0.6876	2.566	0.0512
	10^2	3.679	0.6932	2.551	0.1054
	$3x10^2$	3.582	0.7036	2.520	0.1967
	10^3	3.372	0.7290	2.458	0.3645
	$3x10^3$	3.085	0.7726	2.384	0.5816
	10^4	2.704	0.8367	2.262	0.8248
Nominal	30	3.119	0.6896	2.151	0.0412
	10^2	3.022	0.7027	2.123	0.0846
	$3x10^2$	2.784	0.7477	2.082	0.1582
	10^3	2.759	0.7538	2.079	0.3073
	$3x10^3$	2.648	0.7786	2.062	0.5161
	10^4	2.375	0.8423	2.001	0.7750
Hard	30	2.647	0.7211	1.909	0.0355
	10^2	2.632	0.7244	1.906	0.0742
	$3x10^2$	2.603	0.7310	1.903	0.1425
	10^3	2.536	0.7467	1.894	0.2785
	$3x10^3$	2.419	0.7760	1.877	0.4752
	10^4	2.222	0.8270	1.837	0.7382

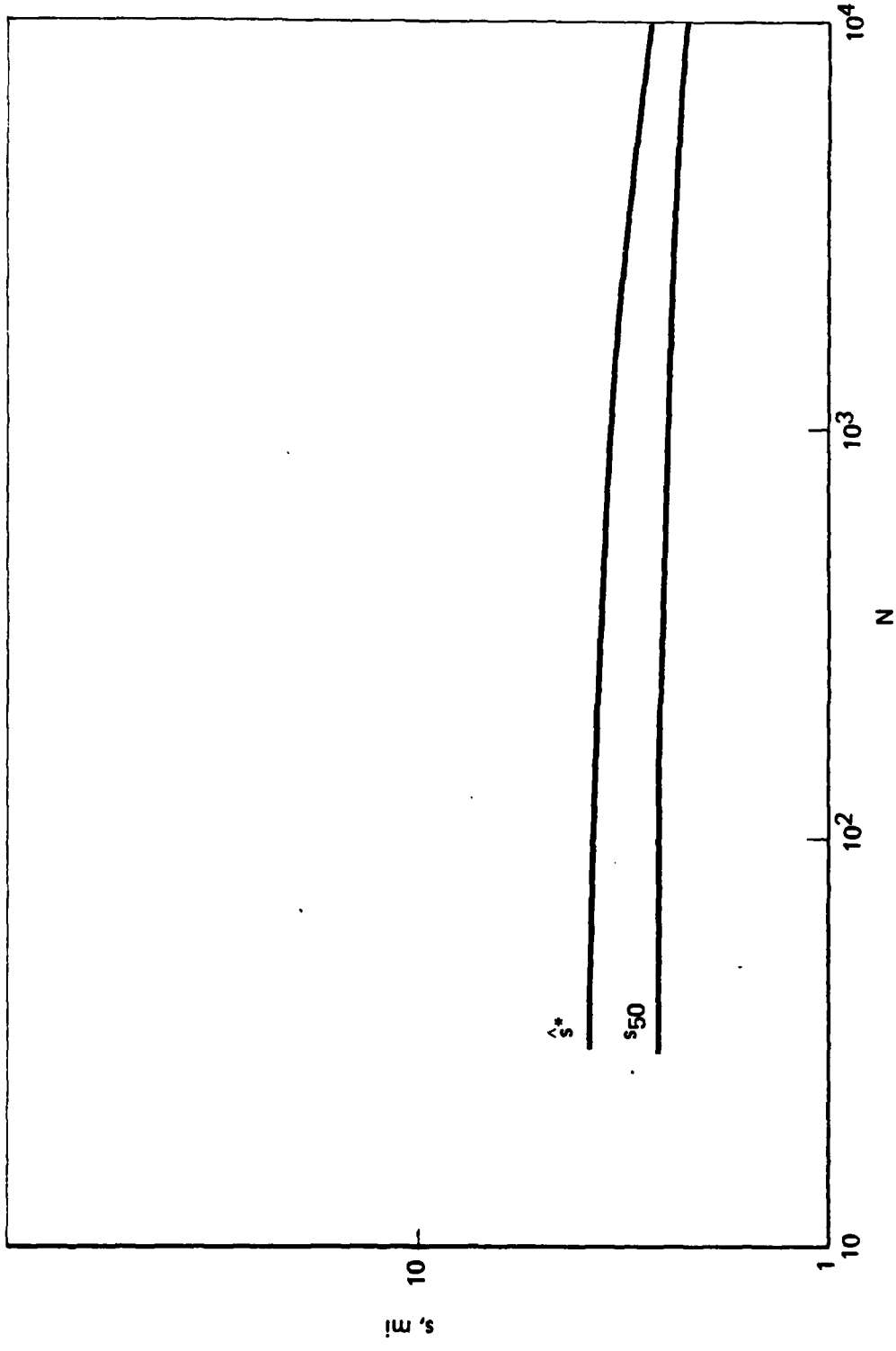

Figure 5. $\hat{s}^*$ and s_{50} vs N for Soft Posture

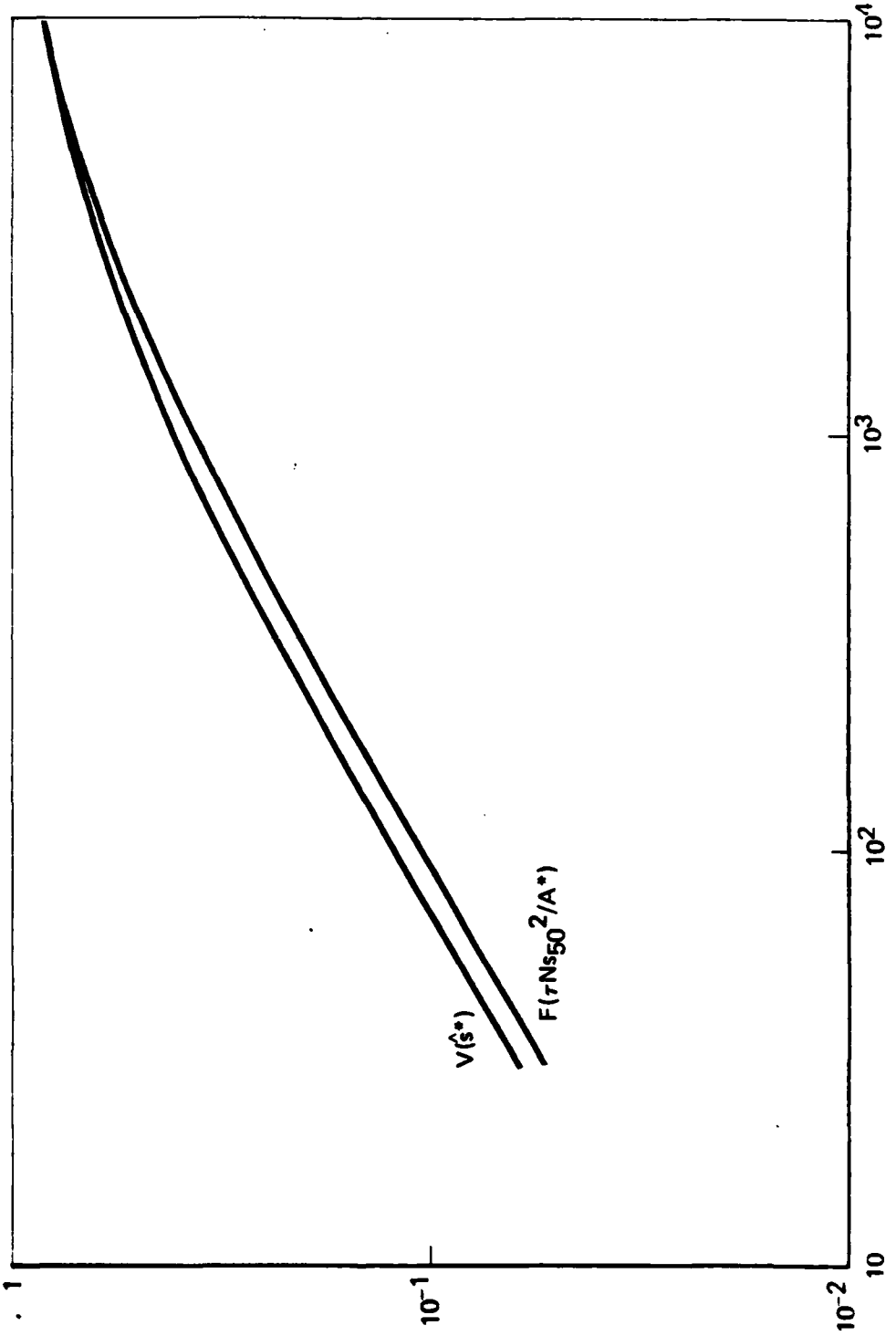

Figure 6. $V(\hat{s}^*)$ and $F(\tau Ns_{50}^2/A^*)$ vs N for Soft Posture

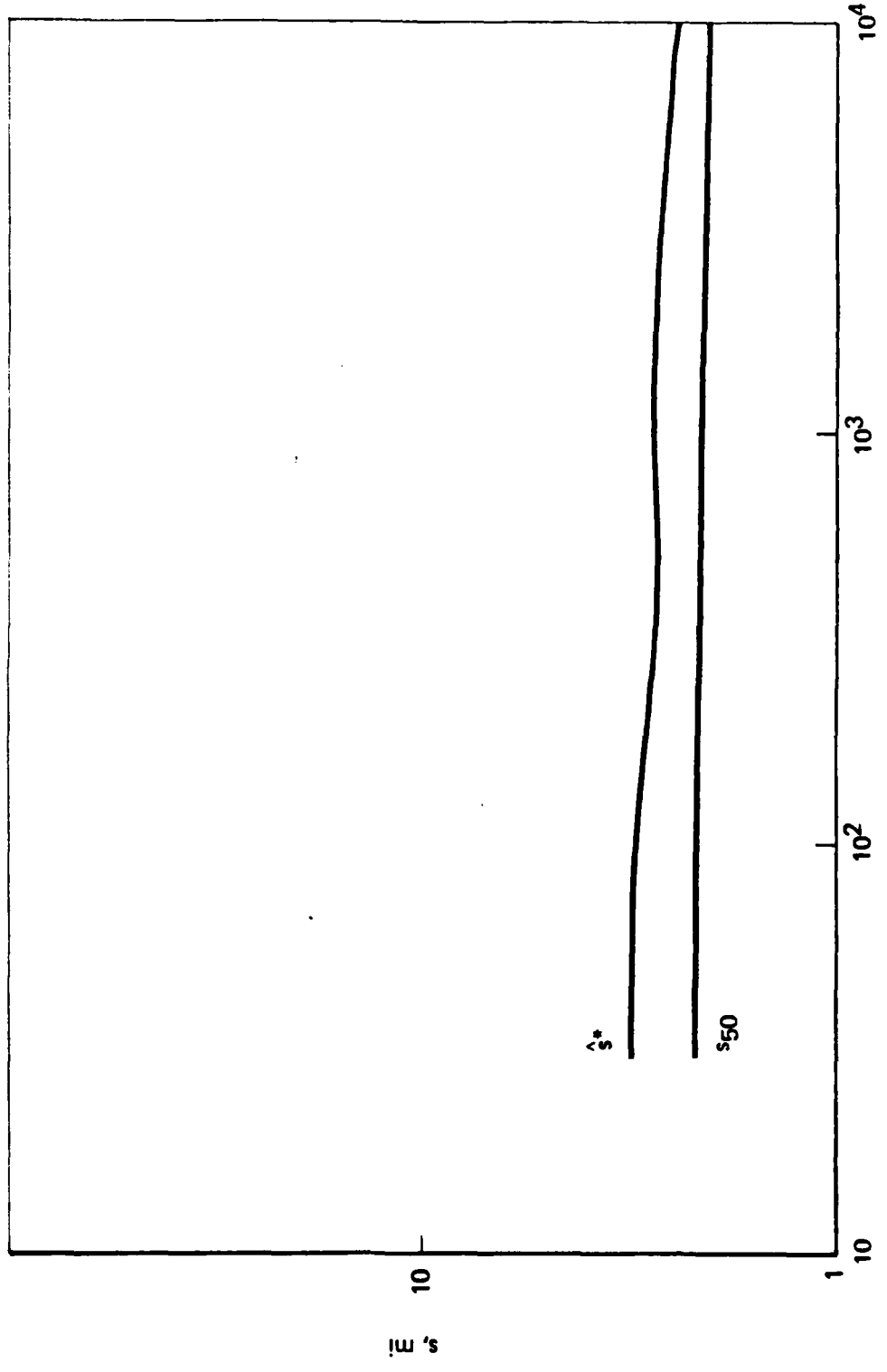

Figure 7. $\hat{s}^*$ and s_{50} vs N for Nominal Posture

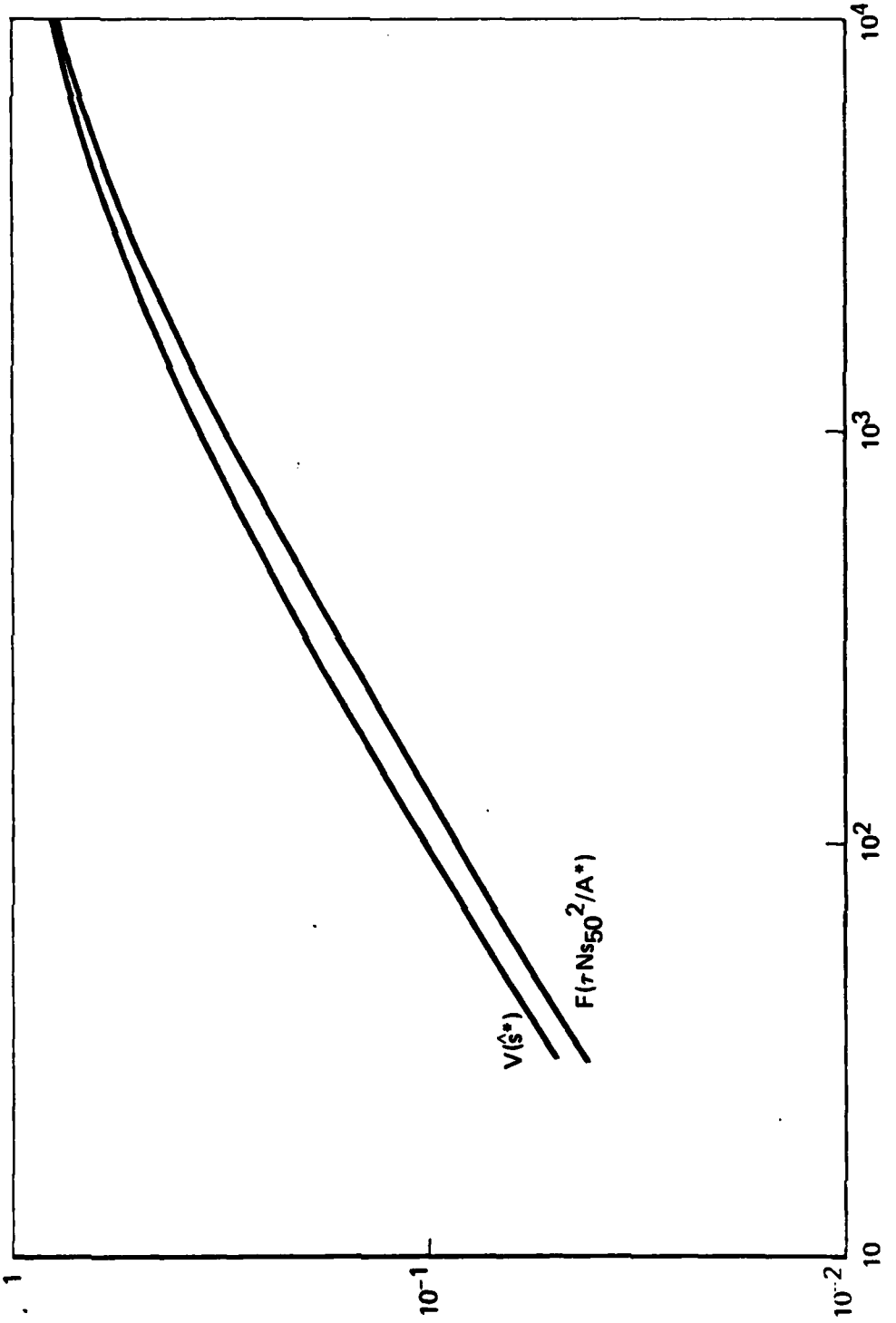

Figure 8. $V(\hat{s}^*)$ and $F(\tau Ns_{50}{}^2/A^*)$ for Nominal Posture

Figure 9. $\hat{s}^*$ and s_{50} vs N for Hard Posture

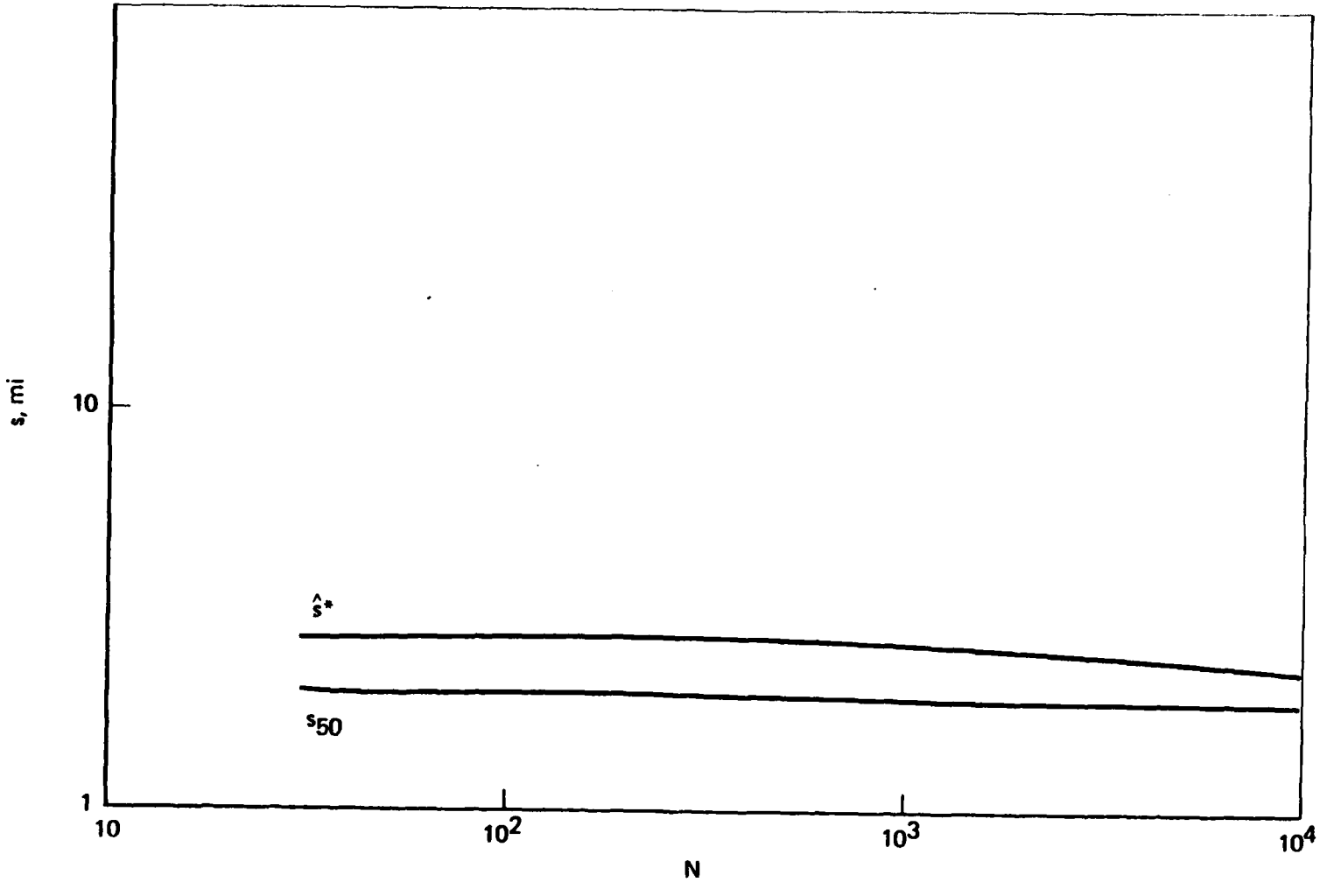

Figure 10. $V(\hat{s}^*)$ and $F(\tau N s_{50}^2/A^*)$ vs N for Hard Posture

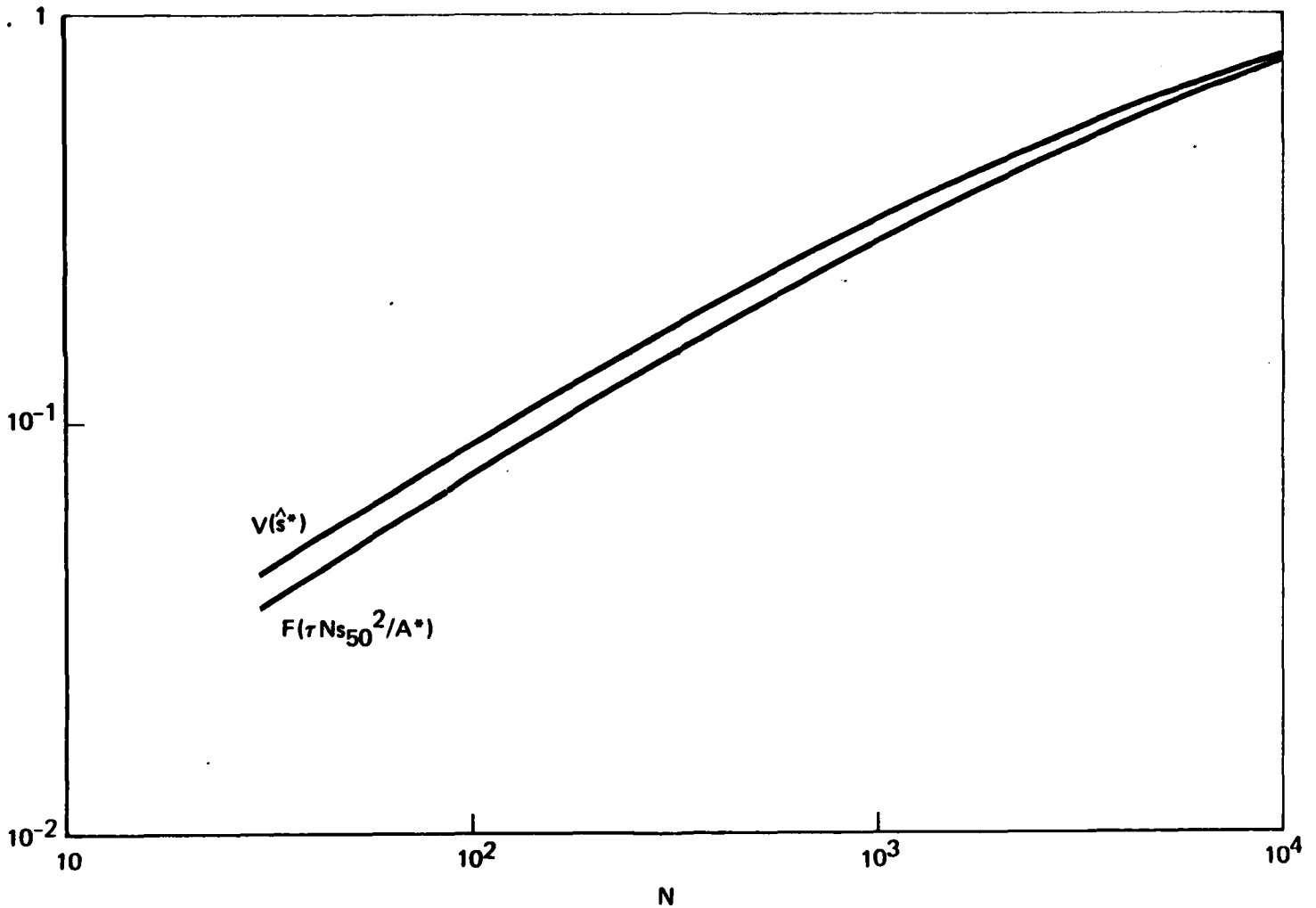

Table 7

Effective Damage Distance and Overpressure for Three Hardness Postures

N	s_{50}, mi. for			$\Delta p_{s,50}$, psi for		
	Soft Posture	Nominal Posture	Hard Posture	Soft Posture	Nominal Posture	Hard Posture
30	2.566	2.151	1.909	6.11	8.46	10.63
10^2	2.551	2.123	1.906	6.18	8.67	10.65
$3x10^2$	2.520	2.082	1.903	6.31	9.00	10.69
10^3	2.458	2.079	1.894	6.60	9.02	10.79
$3x10^3$	2.384	2.062	1.877	6.99	9.16	10.97
10^4	2.262	2.001	1.837	7.70	9.71	11.44

Since $\Delta p_s \sim s^{-n}$ with $n \simeq 2$ for this range of overpressures, the variation of damage overpressure is approximately twice that of the damage distance. However, the variation of both is relatively small. For distributions which are flatter than the distribution $F = F_o$ employed here, the variation is even less. We have shown (cf. Ref. 1) that a defense-conservative upper bound on s_{50} is obtained by taking

$$s_{50} = \left(s_{50,eff}\right)_{lim} = \left[\sum_{j=1}^{M} \alpha_j \, s_{50,j}^2\right]^{1/2} \qquad (36)$$

Substitution of values from Table 3 into Equation 36 gives s_{50} = 2.625 mi., 2.316 mi. and 1.936 mi. for the soft, nominal, and hard postures considered

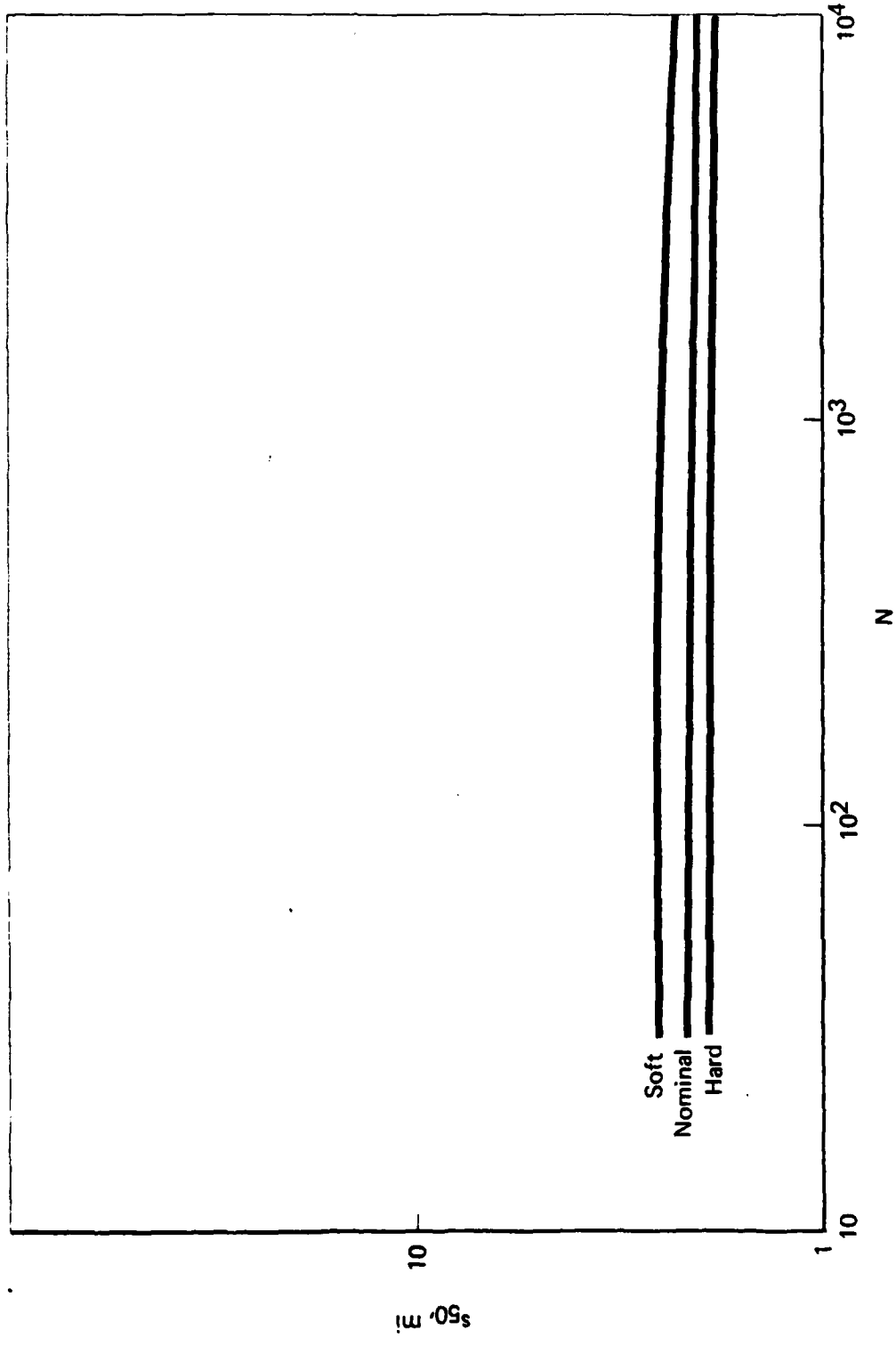

Figure 11. s_{50} vs N for Three Postures

Figure 12. $\Delta p_{s,50}$ vs N for Three Postures

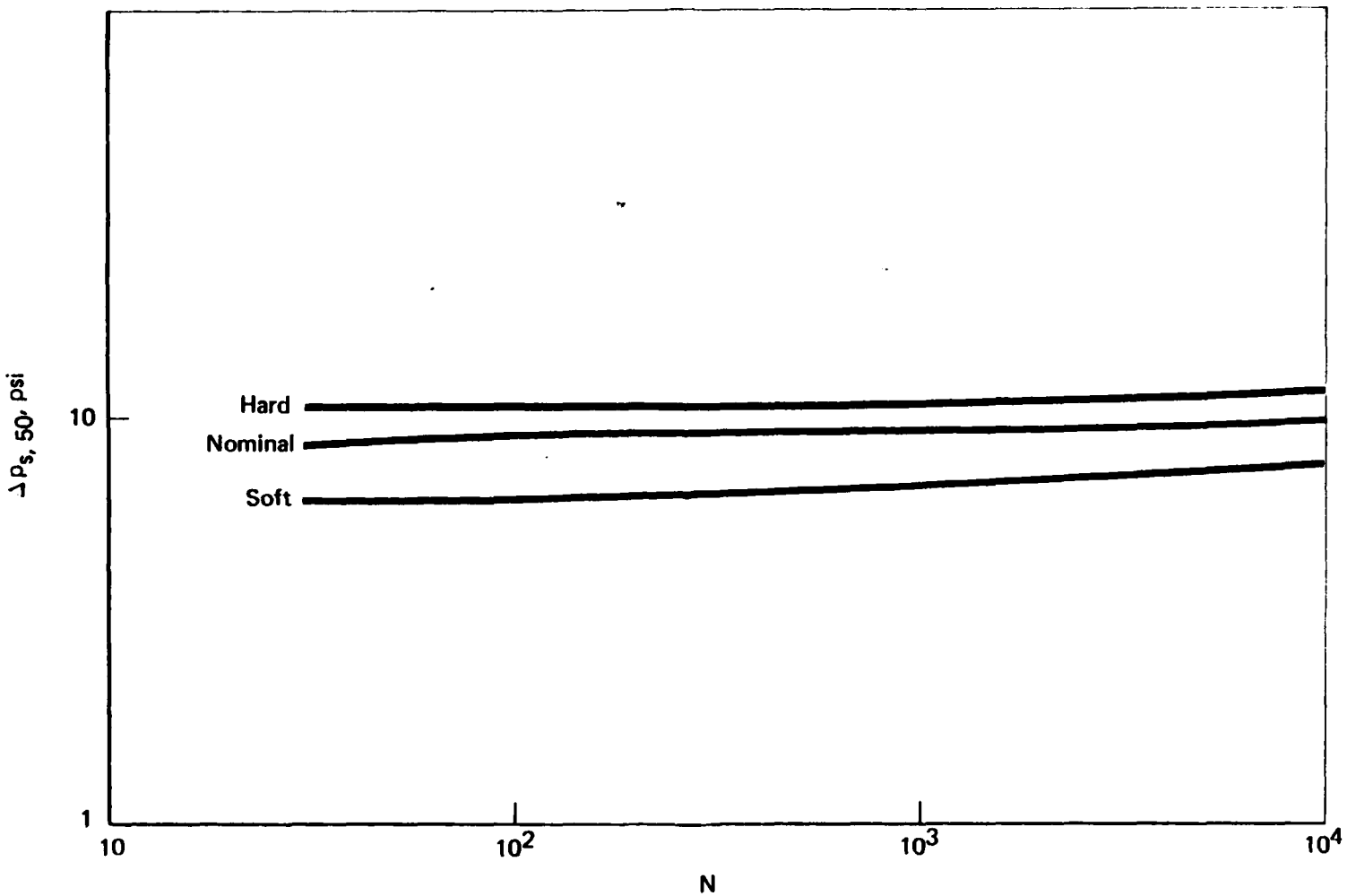

here, with corresponding values for $\Delta p_{s,50}$ of 5.9 psi, 7.4 psi, and 10.3 psi, respectively. Comparison of these values with those tabulated in Table 7 shows that Equation 36 provides a rather good approximation to s_{50} and hence to $\Delta p_{s,50}$. For many applications requiring a defense-conservative estimate, the simplicity of Equation 36 in determining s_{50} and $\Delta p_{s,50}$ outweighs the loss in accuracy.

In sum, we have shown above that our prescription (embodied in Equations 33, 34, 35) for prompt-effects hardness and casualties produces stable, relatively invariant values of effective hardness and approximates closely the "exact" maximum number of casualties achievable.

2.3 Parametric Characterization of Relocation

It is clear, from both common sense and from the precise results of Equation 23, that passive defense measures are perforce combinations of the generic techniques of hardening and dispersion. We have discussed above the characterization of hardness, and now turn to considering dispersion. Special interest attaches to relocation schemes wherein people are evacuated to locations where at least some people already reside. In this subsection we present a parametric characterization of such relocation policies. We first present results for relocation within a single region and then in view of these results, consider nationwide relocation with "self-contained" relocation of individual regions.

Our discussion of relocation is couched in terms of the distributions (rank-ordered by population density and presenting cumulative population versus cumulative area) defined by the spatial distributions of population before and after relocation. Unless otherwise noted, we take the rank-ordered distribution of residential (i.e., pre-relocation) population in each region to be given by Equations 1 and 29 (i.e., by $F = F_o$ with $\lambda = 0.63$) with $A_{occ} = 10A^*$; thus each region is characterized by its total population, Ω_{tot}, and characteristic area, A^*. Since $F_o(10) = 0.986$, use of F_o with $A_{occ} = 10\ A^*$ implies that 1.4 percent of the population lives "outside the populated area". Although this fact is clearly not truly meaningful, it suggests that some caution must be exercised in defining relocated populations in terms of F_o. We adopt the convention that only the $10A^*$ region containing $F_o(10) = 98.6$ percent of the total population is a candidate for receiving evacuees. Moreover, we recognize, within the populated area, three regions corresponding to decreasing ranges of population density for residential population: evacuation region, from which at least some, and generally most, people are relocated; buffer region, neither into nor out of which relocation occurs; potential-host region, i.e., the populated area remainder which is a candidate for receiving evacuees. We distinguish between the potential-host region, so defined, and the host region, which is the region which actually receives evacuees; if the two regions coincide, then the hosting is said to be complete.

Relocation reduces vulnerability insofar as the rank-ordered distribution corresponding to the relocated population is flatter than the

original distribution. The population density is lessened in the evacuation region, is unchanged in the buffer region, and necessarily is increased in the host region. Hence the key to achieving a relatively flat distribution for the relocated population is control of the post-relocation population density within the host region. We therefore consider relocation schemes wherein the population density in the host region is constrained not to exceed a prescribed value, ω^*. A further, pragmatic restriction arises from the finite capacity of the host region to accomodate evacuees; an index of this restriction is the hosting-ratio $\hat{K}$ defined, for any portion of the host region, by

$$\hat{K} = \frac{\text{population after receiving evacuees}}{\text{population before receiving evacuees}} \tag{37}$$

We consider relocation schemes wherein the hosting-ratio in the host region is constrained not to exceed a prescribed value, $\hat{K}^*$.

We now summarize the resulting definition of relocation schemes which evacuate people to locations where at least some people already reside: i) the evacuation region consists of the most densely populated area of $\hat{A}$, and the fraction γ of the population of the evacuation region is relocated; ii) the buffer region consists of the locations where the residential population density is less than in the evacuation region, but greater than ω^*;

iii) within the potential-host region, the locations with the highest residential population density receive as many evacuees as possible, subject to the constraints that the population density after relocation not exceed ω^* and that the hosting ratio not exceed $\hat{K}^*$. The buffer region is represented before relocation by the portion of $F = F_o$ extending from $A = \hat{A}$ to $A = \hat{\hat{A}}$ where, in view of Equation 2,

$$\frac{\Omega_{tot}}{A^*} F'\left(\frac{\hat{\hat{A}}}{A^*}\right) = \omega^* \tag{38}$$

Likewise, the potential-host region is represented before relocation by two portions of $F = F_o$ extending from $A = \hat{\hat{A}}$ to $\tilde{A}$ and from $A = \tilde{A}$ to $A = 10A^*$, respectively, where $\tilde{A}$ is given by

$$\frac{\Omega_{tot}}{A^*} F'\left(\frac{\tilde{A}}{A^*}\right) = \frac{\omega^*}{\hat{K}^*} \tag{39}$$

Clearly, the portion extending from $\hat{\hat{A}}$ to $\tilde{A}$ is limited, after relocation, by the constraint that the population density not exceed ω^*, while the portion extending from $\tilde{A}$ to $10A^*$ is limited by the constraint that the hosting-ratio not exceed $\hat{K}^*$. (Ref. 1 illustrates this generic relocation scheme in a single specific example characterized by taking the region to be the entire nation, $\hat{A} = 1.0A^*$, $\gamma = 0.8$, $\omega^* = 10^3$ people/mi^2, $\hat{K}^* = 7$; the resulting relocated distribution is denoted F_{con}.)

For a given ω^* and $\hat{K}^*$, the potential-host region has a maximum hosting capacity (i.e., excess of population which can be contained over and above the residential population). This maximum capacity occurs for complete hosting and is given by

$$\text{capacity} = \omega^*[\tilde{A}-\hat{\hat{A}}] + \hat{K}^*\Omega_{tot}\left[F(10)-F\left(\frac{\tilde{A}}{A^*}\right)\right] - \Omega_{tot}\left[F(10)-F\left(\frac{\hat{\hat{A}}}{A^*}\right)\right] \quad (40)$$

In dimensionless form we have this capacity (normalized by total population) as Γ where, from Equations 38, 39, 40

$$\Gamma = F'\left(\frac{\hat{\hat{A}}}{A^*}\right)\left[\frac{\tilde{A}}{A^*} - \frac{\hat{\hat{A}}}{A^*}\right] + \hat{K}^*\left[F(10)-F\left(\frac{\tilde{A}}{A^*}\right)\right] - \left[F(10)-F\left(\frac{\hat{\hat{A}}}{A^*}\right)\right] \quad (41)$$

In view of Equations 38 and 39, we also have

$$\Gamma = \hat{K}^*\left\{F'\left(\frac{\tilde{A}}{A^*}\right)\left[\frac{\tilde{A}}{A^*} - \frac{\hat{\hat{A}}}{A^*}\right] + F(10)-F\left(\frac{\tilde{A}}{A^*}\right)\right\} - \left[F(10)-F\left(\frac{\hat{\hat{A}}}{A^*}\right)\right] \quad (42)$$

The hosting demand (i.e., the additional population to be relocated within the host region) is, of course, simply the number of evacuees. In dimensionless

terms, the demand (normalized by total population) is denoted S and given by

$$S = \gamma F(\frac{\hat{A}}{A^*}) \tag{43}$$

In order for the relocation to be feasible, the hosting capacity must exceed the hosting demand, i.e.,

$$\Gamma \geq S \tag{44}$$

We now investigate the conditions for which this fundamental inequality is satisfied. We restrict attention to relocations for which there is no buffer region, so that $\hat{A} = \hat{\hat{A}}$; this serves both to reduce the already large number of parameters and to create the maximum possible hosting demand. (The results presented below are readily extended to include a finite buffer region; specific buffer regions considered in the past are difficult to characterize in intrinsic terms, but generally have relatively small total population.) Our approach is to characterize relocations with complete hosting; the resulting post-relocation rank-ordered distributions are denoted by G (to avoid confusion with the pre-relocation distribution $F = F_o$).

We proceed by first determining the minimum permissible ω^* for given $\hat{K}^*$ and γ. Determining this minimum permissible ω^* is equivalent (via

Equation 38) to determining the maximum permissible $\hat{\tilde{A}}$ and hence is equivalent (via Equation 39) to determining the maximum permissible $\tilde{A}$. Of the various alternative ways to achieve these equivalent ends, perhaps the simplest is interpreted as an iterative procedure (with convergence guaranteed by the fact that the procedure is demonstrably equivalent to inverting a monotonic function) wherein one i) picks a value of $\tilde{A}$, ii) thereby determines $\hat{\tilde{A}}$ since Equations 38 and 39 imply that

$$F'(\frac{\hat{\tilde{A}}}{A^*}) = \hat{K}^* F(\frac{\tilde{A}}{A^*}) \tag{45}$$

iii) thereby determines Γ from Equation 41 or 42, iv) compares Γ with S determined from Equation 43 with $\hat{A} = \hat{\tilde{A}}$, v) iterates to obtain $\Gamma = S$. We denote the results in terms of the parameters $\hat{\tilde{a}}$ and $\tilde{a}$ which give the maximum permissible values of $\hat{\tilde{A}}$ and $\tilde{A}$ via

$$\hat{\tilde{a}} = \frac{\text{maximum permissible } \hat{\tilde{A}}}{A^*} \tag{46}$$

$$\tilde{a} = \frac{\text{maximum permissible } \tilde{A}}{A^*} \tag{47}$$

It obviously follows that

$$\text{minimum permissible } \omega^* = \frac{\Omega_{tot}}{A^*} F'(\hat{\tilde{a}}) = \hat{K}^* \frac{\Omega_{tot}}{A^*} F'(\tilde{a}) \tag{48}$$

The results are summarized in Tables 8 and 9 and Figures 13, 14, and 15. Tables 8 and 9 list critical values of hosting parameters (e.g., $\hat{\hat{a}}$, $\tilde{a}$, and functions thereof) as functions of $\hat{K}^*$ for $\gamma = 1.0$ and 0.8, i.e., for 100 percent and 80 percent evacuation, respectively. Figures 13 plots the minimum permissible hosting population density ω^* as a function of $\hat{K}^*$ for $\gamma = 1.0$ and 0.8; alternatively, Figure 13 depicts the boundary in population-density/hosting-ratio space between feasible and infeasible relocations. In like fashion, Figures 14 and 15 present the variation with $\hat{K}^*$ of the maximum evacuated population, $\gamma F(\hat{\hat{a}})$, and maximum evacuation area, $\hat{\hat{a}}$, respectively; these Figures may also be interpreted as defining boundaries in the appropriate parameter space. We note the results that, for $\hat{K}^* = 7$, then the minimum permissible hosting population density ω^* is 0.1741 Ω_{tot}/A^* and 0.1433 Ω_{tot}/A^* for $\gamma = 1.0$ and $\gamma = 0.8$, respectively; the analogous values of maximum evacuated population are 0.6945 Ω_{tot} and 0.5860 Ω_{tot}, while the analogous values of maximum evacuated area are 1.3106 A^* and 1.5511 A^*, respectively. We further note the consequence that for γ - 0.8 and $\hat{K}^* = 7$, a hosting population density $\omega^* = 10^3$ people/mi^2 implies a feasible relocation if, and only if, Ω_{tot}/A^* is less than $(0.1433)^{-1}\ 10^3$ people/mi^2 = 6.98×10^3 people/mi^2 $\simeq$ 7×10^3 people/mi^2.

It is apparent from Figures 13 through 15 that for hosting-ratios larger than 6 to 8, the critical values of population density, evacuated population and evacuation area tend to flatten out; thus the dependence upon hosting-ratio is weak, once the hosting-ratio reaches approximately 7. Additional insight into the behavior of the relocation is obtained by examining how the population after relocation is distributed among the three (mutually exclusive and

Table 8

Critical Values of Hosting Parameters for 100% Evacuation

$\hat{K}^*$	$\tilde{a}$	$F(\tilde{a})$	$F'(\tilde{a})$	$\hat{\hat{a}}$	$F(\hat{\hat{a}})$	$F'(\hat{\hat{a}})$	Γ	$\Gamma/F(\hat{\hat{a}})$
2	0.9582	0.6222	0.2418	0.4237	0.4413	0.4836	0.4413	1.0000
3	2.0113	0.7884	0.1029	0.7377	0.5620	0.3088	0.5620	1.0000
4	2.8723	0.8569	0.0610	0.9489	0.6200	0.2441	0.6199	1.0000
5	3.5863	0.8931	0.0420	1.1018	0.6546	0.2099	0.6546	1.0000
6	4.1928	0.9152	0.0314	1.2184	0.6778	0.1887	0.6778	1.0000
7	4.7186	0.9299	0.0249	1.3106	0.6945	0.1741	0.6945	1.0000
8	5.1818	0.9403	0.0204	1.3852	0.7071	0.1636	0.7071	1.0000
9	5.5948	0.9481	0.0173	1.4467	0.7169	0.1556	0.7169	1.0000
10	5.9670	0.9541	0.0149	1.4981	0.7247	0.1493	0.7247	1.0000
15	7.4090	0.9707	0.0088	1.6609	0.7476	0.1318	0.7476	1.0000
20	8.4238	0.9783	0.0062	1.7388	0.7576	0.1245	0.7576	1.0000

Table 9

Critical Values of Hosting Parameters for 80% Evacuation

$\hat{K}^*$	$\tilde{a}$	$F(\tilde{a})$	$F'(\tilde{a})$	$\hat{\hat{a}}$	$F(\hat{\hat{a}})$	$F'(\hat{\hat{a}})$	Γ	$\Gamma/F(\hat{\hat{a}})$
2	1.1508	0.6646	0.2006	0.5408	0.4928	0.4012	0.3942	0.8000
3	2.3153	0.8168	0.0846	0.9116	0.6107	0.2538	0.4885	0.8000
4	3.2408	0.8772	0.0501	1.1528	0.6650	0.2002	0.5320	0.8000
5	3.9967	0.9087	0.0344	1.3236	0.6967	0.1722	0.5574	0.8000
6	4.6325	0.9277	0.0258	1.4516	0.7177	0.1550	0.5741	0.8000
7	5.1795	0.9403	0.0205	1.5511	0.7325	0.1433	0.5860	0.8000
8	5.6580	0.9492	0.0169	1.6304	0.7435	0.1349	0.5948	0.8000
9	6.0825	0.9558	0.0143	1.6948	0.7520	0.1285	0.6016	0.8000
10	6.4632	0.9608	0.0124	1.7478	0.7587	0.1237	0.6070	0.8000
15	7.9224	0.9749	0.0074	1.9080	0.7774	0.1104	0.6219	0.8000
20	8.9333	0.9812	0.0053	1.9757	0.7847	0.1054	0.6277	0.8000

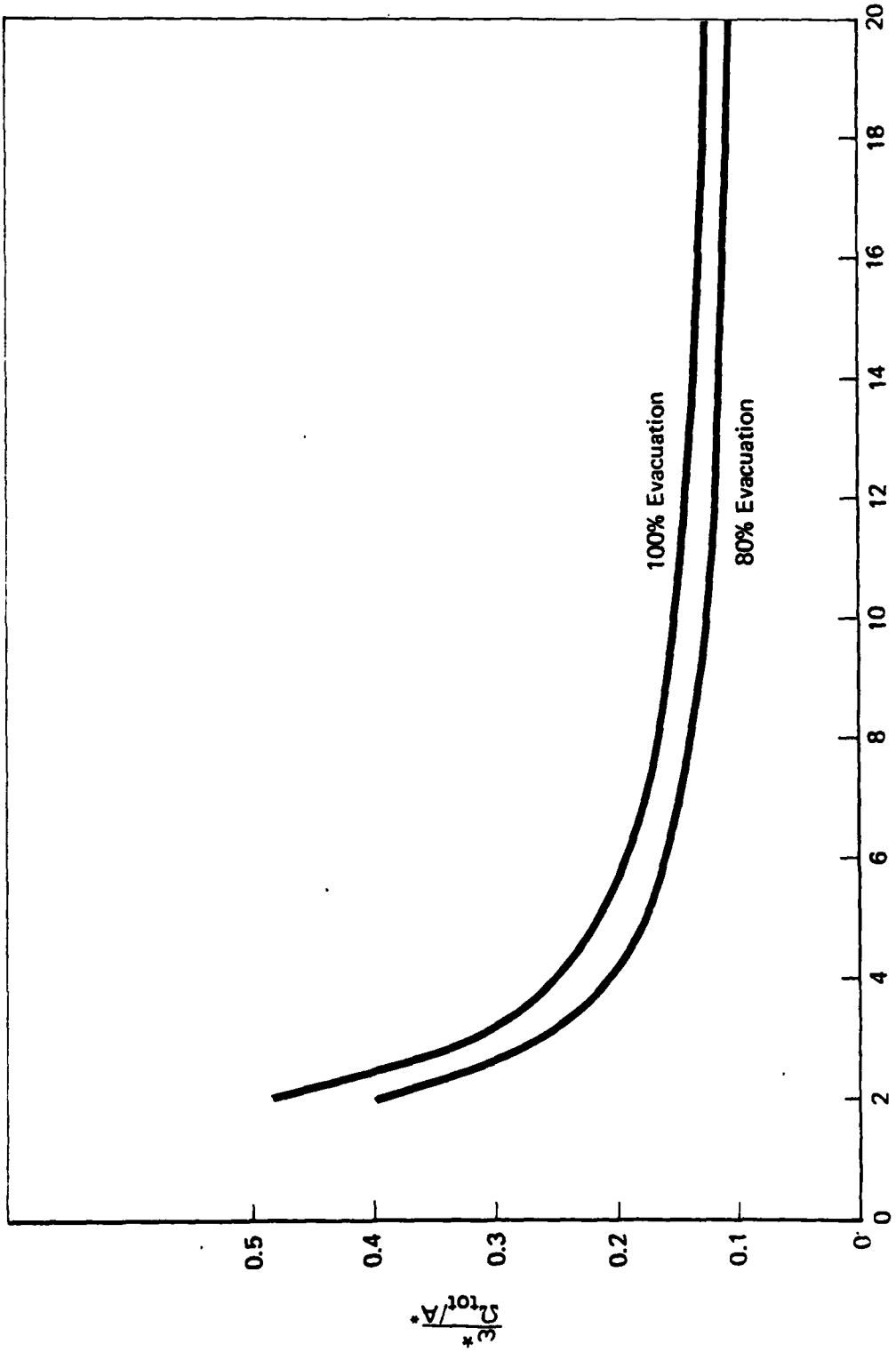

Figure 13. Minimum Permissible Hosting Population Density vs Hosting-Ratio

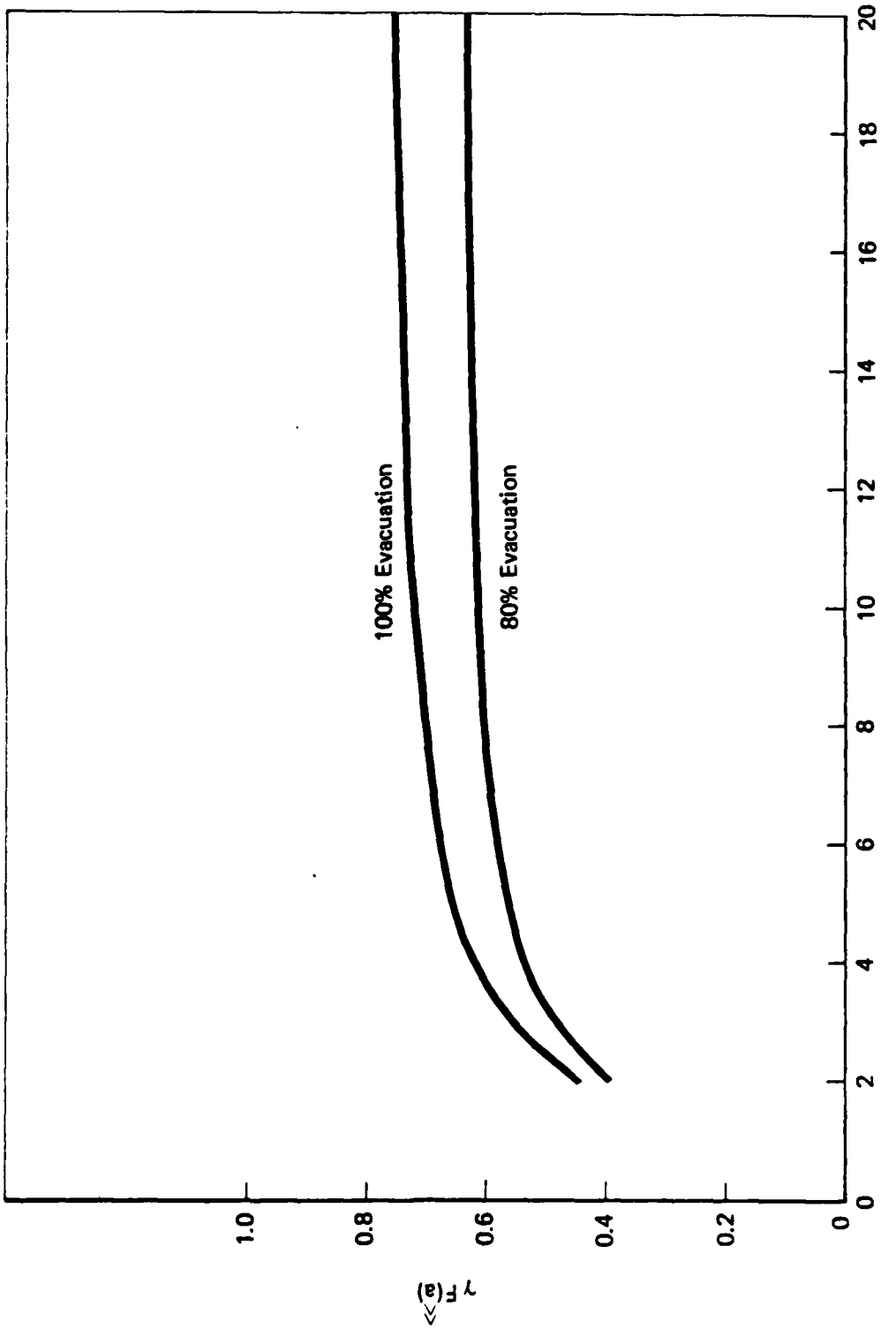

Figure 14. Maximum Permissible Evacuated Population vs Hosting-Ratio

Figure 15. Maximum Permissible Evacuation Area vs Hosting-Ratio

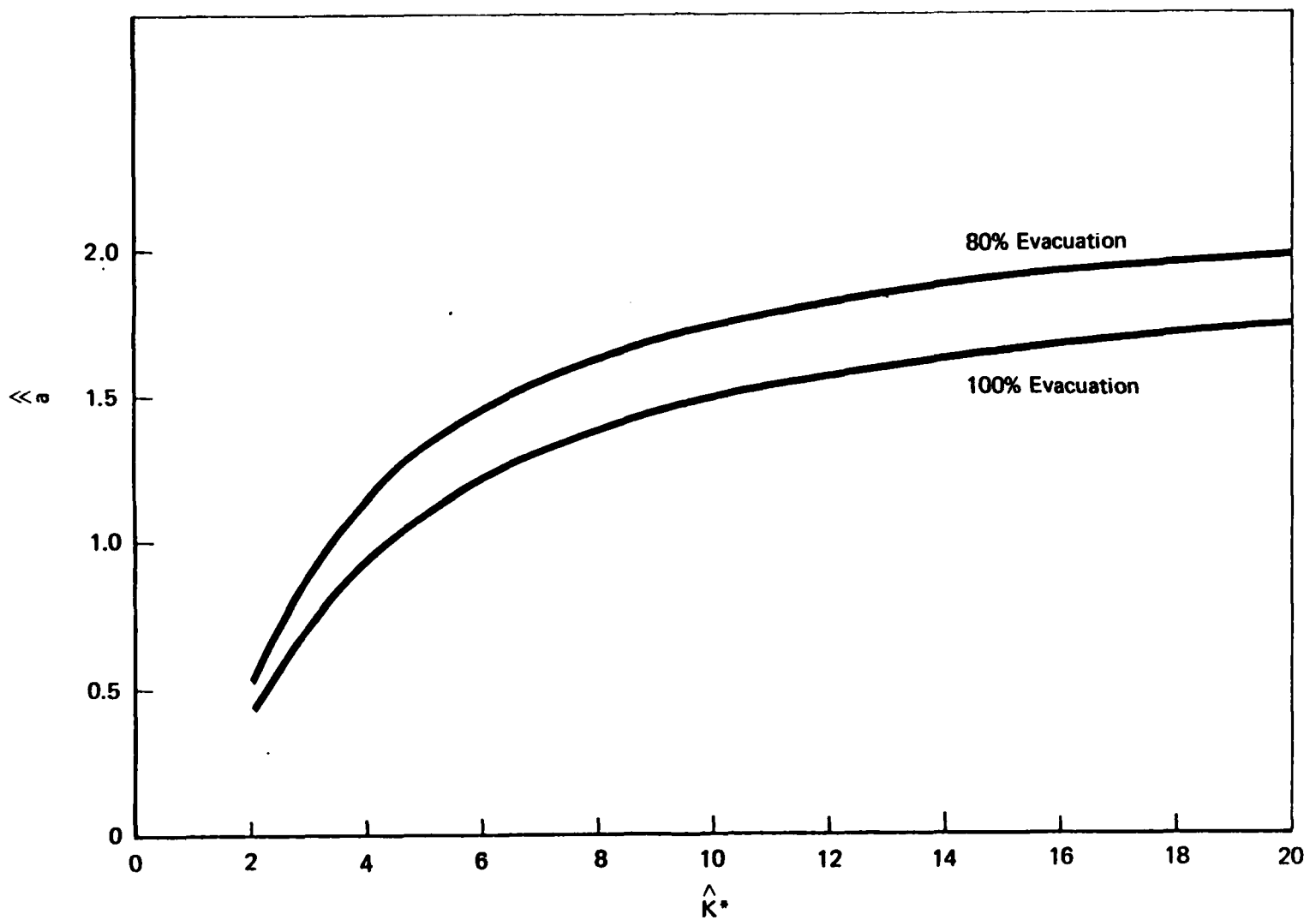

collectively exhaustive) regions: evacuation region, host-region with constant population density, host-region with constant hosting-ratio. Figures 16 and 17 present the population of these three regions as a function of hosting-ratio for $\gamma = 1.0$ and $\gamma = 0.8$, respectively; for $\gamma = 1.0$, the post-relocation population of the evacuation region is, of course, zero. We see from these Figures that the post-relocation population of the evacuation region depends weakly (e.g., varying between 10 and 16 percent for $\gamma = 0.8$) on hosting-ratio, while the post-relocation host region population with constant population density increases steadily with increasing hosting-ratio; necessarily, the remaining population (i.e., host region with constant hosting-ratio) decreases steadily with increasing hosting ratio. Although these breakdowns of the total post-relocation population are instructive, it is even more informative to determine the rank-ordered (by population density) distributions G which are defined by the relocated population.

It is clear that, for complete relocation with $\Gamma = S$, the rank-ordered distribution G begins with that portion of the evacuation region which even after relocation has population density greater than ω^*. The next portion of G has uniform population density ω^*. In rank-ordering the balance of the relocated population (i.e., the remainder of the evacuation region, plus the host region with constant hosting-ratio) it is necessary to recognize that the smallest population density in the evacuation region is $(1-\gamma)\omega^*$, while the smallest population density in the host region is $\hat{K}^*F'(10)\Omega_{tot}/A^*$, where $F'(10) = 3.773 \times 10^{-3}$.

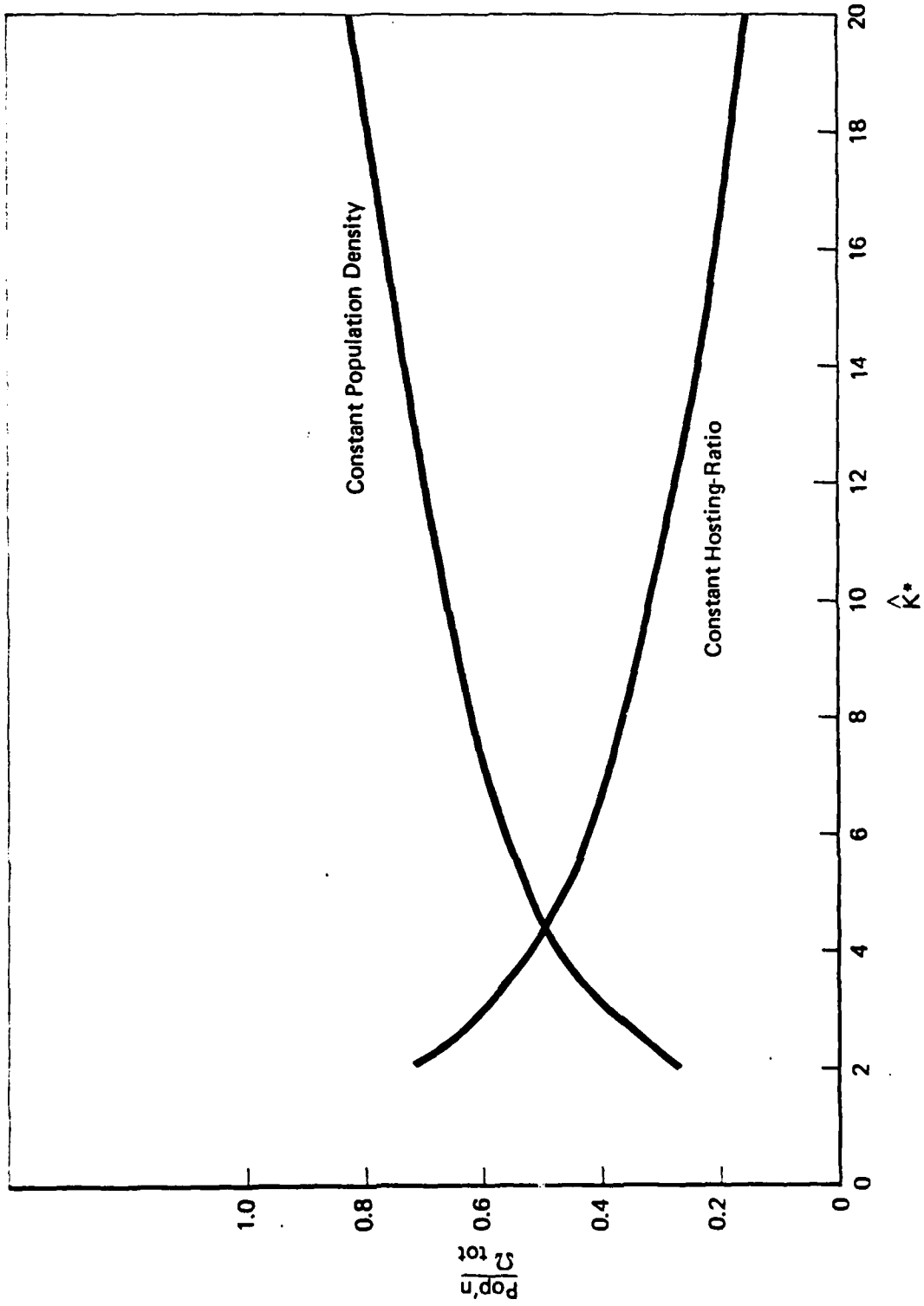

Figure 16. Breakdown of Post-Relocation Population vs Hosting-Ratio for 100% Evacuation

Figure 17. Breakdown of Post-Relocation Population vs Hosting-Ratio for 80% Evacuation

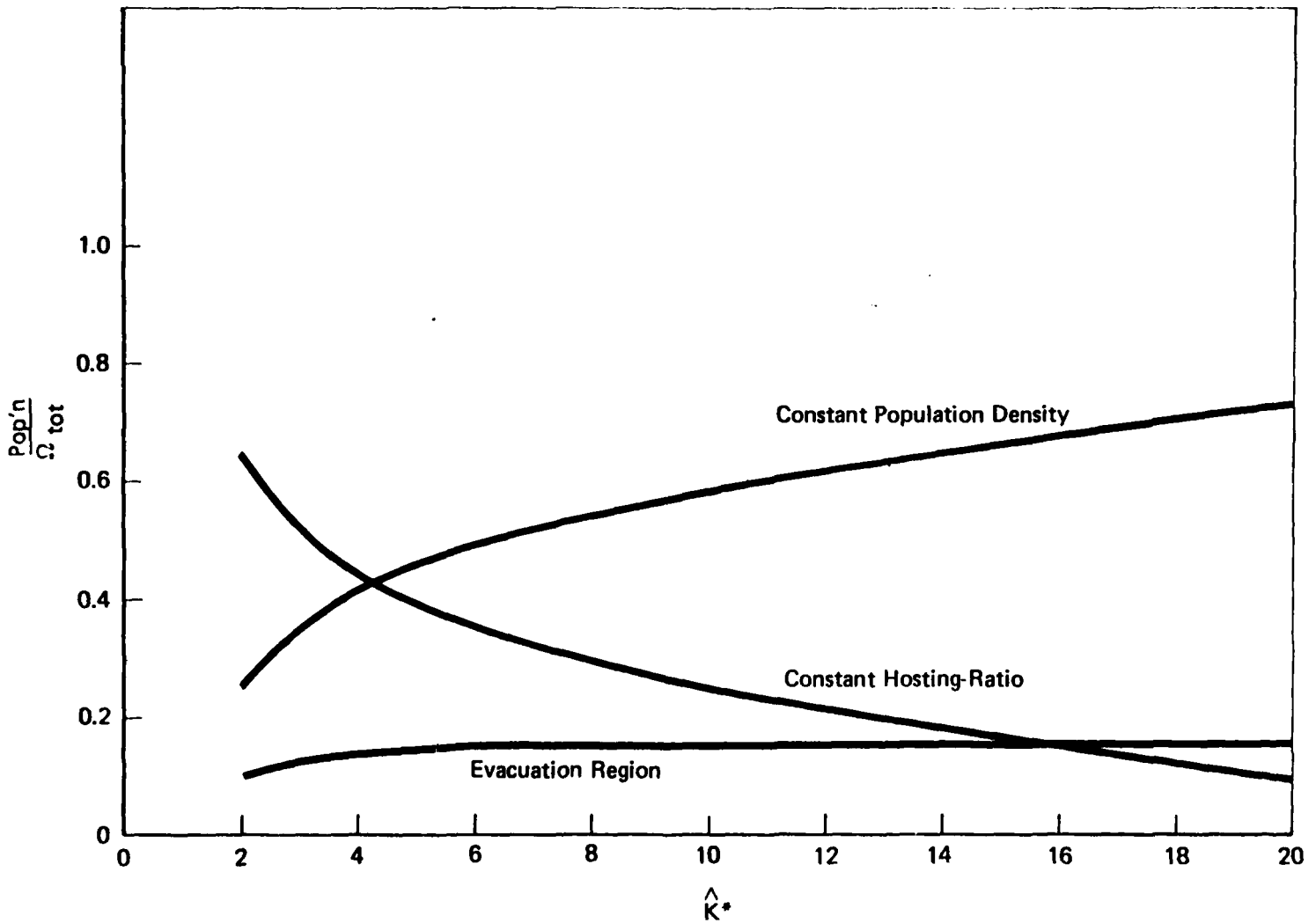

For a given γ, the result is that for sufficiently small hosting-ratio $\hat{K}^*$, the least densely populated cells are in the host region, i.e., $\hat{K}^*F'(10)\Omega_{tot}/A^* < (1-\gamma)\omega^*$; for sufficiently large hosting-ratio, the converse holds. As may be seen from Table 9 for $\gamma = 0.8$, the transition occurs for $\hat{K}^*$ between 7 and 8. Thus for 80 percent evacuation, the least densely populated portion of the relocated population is located in the host region for $\hat{K}^* \leq 7$ and in the evacuation region for $\hat{K}^* \geq 8$. In general, then, after the portion with constant population density ω^*, the rank-ordered distribution G has a portion containing people from the evacuation region and from the host region with population density between ω^* and the greater of the two minimum population densities of these two regions. The final portion of G then contains the balance of the residents of the region with smaller minimum population density. The precise, quantitative characterization of the distribution G is presented in Appendix A, which may be consulted for details and numerical examples.

The preceding discussion has considered a single region exclusively and the relocation of the region's population within the region itself. Such regionally self-contained relocations are an integral part of relocation on a larger (e.g., national) scale. Therefore, the results presented above have significant consequences for larger scale relocation. For example, we have seen above that for 80 percent evacuation and a critical hosting-ratio of 7 then a critical population density of 1,000 people/mi^2 implies a feasible relocation if and only if the region's Ω_{tot}/A^* is less than 7.0×10^3 people/mi^2. Consequently, (from the demographic statistics of Table 3, Ref. 1) we see

that relocation with these values of the hosting parameters is feasible for the entire CONUS and for the Midwest (with Ω_{tot}/A^* of 5.7×10^3 and 6.8×10^3 people/mi^2, respectively), but not for the Northeast and California (with Ω_{tot}/A^* of 9.8×10^3 and 10.2×10^3 people/mi^2, respectively). Thus the specific relocation described in Ref. 1 is feasible on a national scale, but has the drawback that residents of the Northeast and California must be relocated outside their own regions. The definition of this specific relocation has been repeated above and can be paraphrased as calling for i) 80 percent evacuation of the locations wherein the residential population density exceeds 1.2×10^3 people/mi^2, ii) a buffer region consisting of residential population with population density between 1.2×10^3 people/mi^2 and $\omega^* = 1.0 \times 10^3$ people/mi^2, iii) a potential host region wherein the population density after relocation does not exceed ω^* and the hosting-ratio does not exceed $\hat{K}^* = 7$.

For the Northeast (with $\Omega_{tot}/A^* = 9.8 \times 10^3$ people/mi^2), the values of $\omega^* = 10^3$ people/mi^2 and $\hat{K}^* = 7$ imply that $\hat{\hat{a}} = 2.028$ and $\tilde{a} = 6.039$; substitution of these values into Equations 41 or 42 gives a maximum capacity of $\Gamma = 0.4293$. However, the evacuation of residential locations with population density greater than 1.2×10^3 people/mi^2 implies that $\hat{A}$ is 1.792 times the characteristic area A^* for the Northeast; hence, from Equation 43, the demand (i.e., the number of evacuees) is 0.6112. Consequently, the demand exceeds the capacity by (0.6112-0.4293) = 0.1819 times the regional population of 54.9 million people; thus 10.0 million residents of the Northeast cannot be relocated within the Northeast. Moreover, the fraction (0.1819/0.6112) = 29.8 percent of the evacuees can't be relocated within the Northeast.

For California, the analogous calculations give the results that $\hat{\hat{a}} = 2.090$, $\tilde{a} = 6.143$, $r = 0.4127$ while $S = 0.6167$ for $\hat{A}$ equal to 1.850 times the regional characteristic area A^*. Consequently, demand exceeds capacity by (0.6167-0.4127) = 0.2040 times the regional population of 21.1 million; thus 4.3 million California residents cannot be relocated within California. Likewise, the fraction (0.2040/0.6167) = 33.1 percent of the evacuees cannot be relocated within California. In sum, then, we see that for both the Northeast and California, some one-fifth of the total regional population and some one-third of the total number of evacuees cannot be relocated within their own region.

We now illustrate how the abstract results derived above can be applied to define a nationwide relocation for which relocation of the Northeast and California is self-contained. We again consider relocation with evacuation fraction $\gamma = 0.8$ and critical hosting-ratio $\hat{K}^*$ of 7; as noted above, hosting-ratios larger than 7 have limited payoff and cause the entire host region to be more densely populated than some portions of the evacuation region. Since the Northeast and California have very nearly the same residential population density Ω_{tot}/A^* ($\approx 10^4$ people/mi^2), we treat them as a single region with total population of 76 million and characteristic area A^* of 7.5×10^3 mi^2, and we consider the remainder of the nation as a second region with total population of 136 million and characteristic area A^* of 30.6×10^3 mi^2; to within roundoff, these values preserve the total population and total occupied areas

of the regions (given in Ref. 1, Table 3, based on DCPA extrapolation of 1970 census data), while taking $A_{occ} = 10A^*$. These values imply that Ω_{tot}/A^* is 10,133 people/mi^2 and 4,444 people/mi^2 for the two regions. By demanding that the relocation of the artificial composite region consisting of the Northeast plus California be self-contained, we obviously guarantee that the relocation of the actual, geographically distinct regions be individually self-contained. From Table 9 (or Figure 13), we find that, for $\gamma = 0.8$ and $\hat{K}^* = 7$, the minimum permissible hosting population density for self-contained relocation is 0.1433 (10,133 people/mi^2) = 1452 people/mi^2 for the Northeast and California. Consequently, a national relocation with $\omega^* = 1452$ people/mi^2 and $\hat{K}^* = 7$ will permit residents of the Northeast and California to be relocated in their own regions, with complete hosting.

The national relocation thus inferred calls for i) evacuating 80 percent of the population in all locations where the residential population density exceeds 1452 people/mi^2, ii) having no buffer region, iii) restricting the population density and hosting-ratio not to exceed 1452 people/mi^2 and 7, respectively, in the host region. By construction, the hosting of the Northeast and California is complete, with parameters given by Table 9. For the region consisting of the balance of the nation, we find that the evacuation region has a residential population of 0.5476 times the total regional population and an area of 0.6919 times the region's characteristic area. Consequently, the number of evacuees is 0.8 (0.5476) = 0.4380 times the regional population.

We find that these evacuees are accomodated in the host region with uniform population density of 1452 people/mi^2 over an area of 2.3107 times the characteristic area of the region. In the composite rank-ordered distribution for the entire (relocated) nation, we find that 4.20 percent of the national population has population density greater than 1452 people/mi^2 and covers an area of 3.22×10^3 mi^2, while 67.07 percent of the national population has population density equal to 1452 people/mi^2 and covers an area of 97.92×10^3 mi^2. The balance of the population (less than 30 percent of the total) is contained in the evacuation region, in the constant hosting-ratio portion of the host region for the Northeast and California, and in the remainder of the potential host region for the rest of the nation; the last of these are at residential population density. We call this rank-ordered distribution F_{SC} and plot it in Figure 18 along with the distribution F_{con} derived earlier (Ref. 1); in plotting Figure 18, we take the characteristic area A* for the nation to be 4×10^4 mi^2 , i.e., the value used earlier in constructing F_{con}. We also include in Figure 18 the distribution $F = F_o$ corresponding to residential population and the absolutely limiting distribution $F = F_\infty$ corresponding to uniform population density over the entire populated area.

It is apparent from Figure 18 that requiring the relocation of the Northeast and California to be self-contained has steepened the rank-ordered distribution of the relocated population. Moreover, by comparison with the irreducible limit of $F = F_\infty$ with its uniform population density of approximately

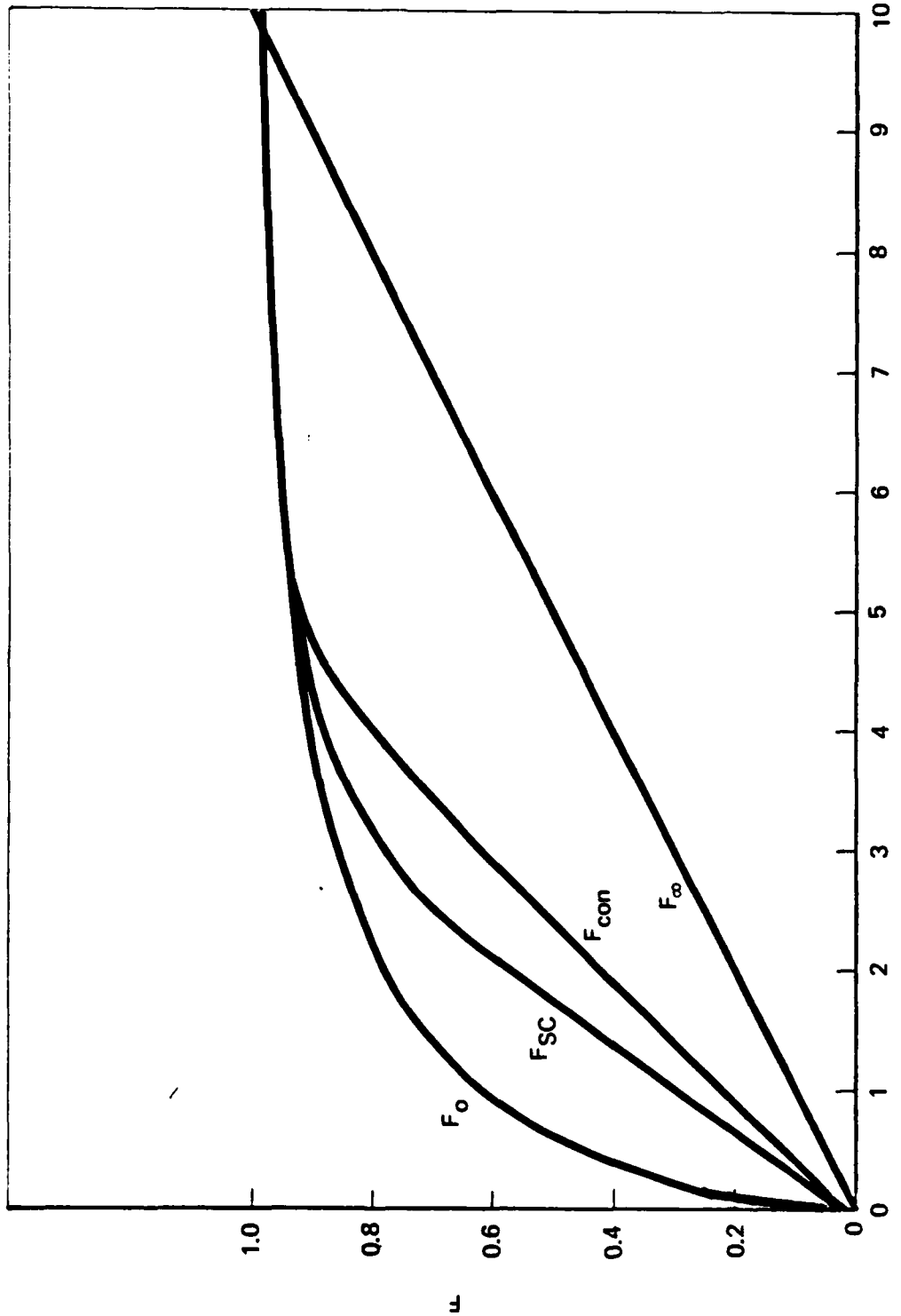

Figure 18. Comparison of Rank-Ordered National Population Distributions

500 people/mi^2, the distributions F_{con} and F_{SC} have the bulk (greater than 70 percent of the national population) at population densities of approximately 1,000 and 1,500 people/mi^2, respectively, i.e., approximately 2 and 3 times the irreducible limit. Despite the idealizations in our derivation of the distributions F_{SC} and F_{con}, it is highly plausible that no rank-ordered nation-wide distribution flatter than something intermediate between F_{SC} and F_{con} can be produced by any realistic relocation scheme which evacuates people to locations where at least some people already reside and which guarantees self-contained relocation for regions of reasonable size. Moreover, the detailed definition of any such relocation scheme must recognize the inherent capacity vs. demand limitations explored above and will be simplified by applying the specific abstract results derived above.

2.4 Applications and Examples

Section 2.1 above has summarized a number of fundamental results concerning the structure of casualty prediction problems. Because of the analytic simplicity of these results, it is straightforward to characterize parametrically the interrelationships among the problem's ingredients. In this subsection, rather than constructing an encyclopedic catalog of such parametric results, we present numerical examples and analytic extensions choosen to illustrate some basic properties of passive defense.

We begin by exploring the relative influence of hardening and dispersion. We consider prompt-effects casualties exclusively; equivalently, we consider combined-effects casualties for populations whose weighted protection factor is large enough to satisfy the condition of Equation 25. We consider airbursts exclusively, optimized for the prompt-effects hardness $\Delta p_{s,50}$. We have seen above that the prompt-effects hardness for the residential population, even in "best available shelter", lies between 5 and 10 psi; we typically take 7 psi as a representative value for the prompt-effects hardness. The spatial arrangement of the population is represented by the distribution F, rank-ordered by population density; we have seen above that $F = F_o$ for the residential population, while the most defense-optimistic F lies between F_{SC} and F_{con} for population relocated to places where at least some people already reside.

Figure 19 (based on Equation 23) presents, as a function of blast-equivalent megatons (i.e., $NY^{2/3}$), defense-conservative estimates of the prompt-effects hardness needed to achieve survivor fractions of 1/2 and 2/3 for the residential and relocated (according to F_{SC} and F_{con}) populations. It is apparent that even for the relocated populations, significant hardness is required for not unreasonable attack sizes. An alternative viewpoint is presented in Figure 20 (based on Equation 5) which plots a defense conservative estimate of fatalities as a function of blast-equivalent megatons for a population with $\Delta p_{s,50} = 7$ psi and with spatial distribution corresponding to

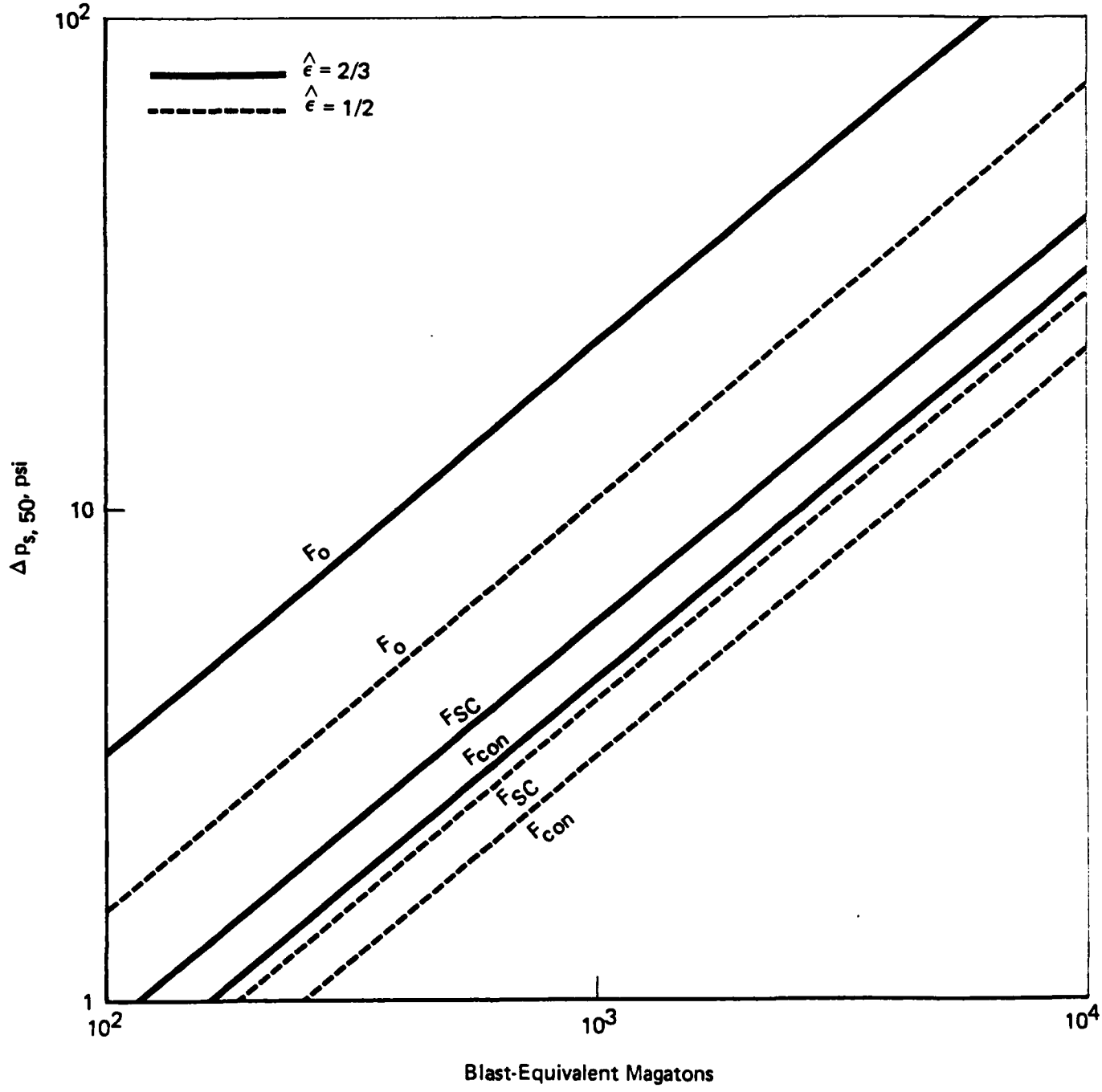

Figure 19. Prompt-Effects Hardness for Specified Survivor-Fraction, For Residential and Relocated Populations

Figure 20. Fatalities vs Attach Size for 7-psi Population, Residential and Relocated

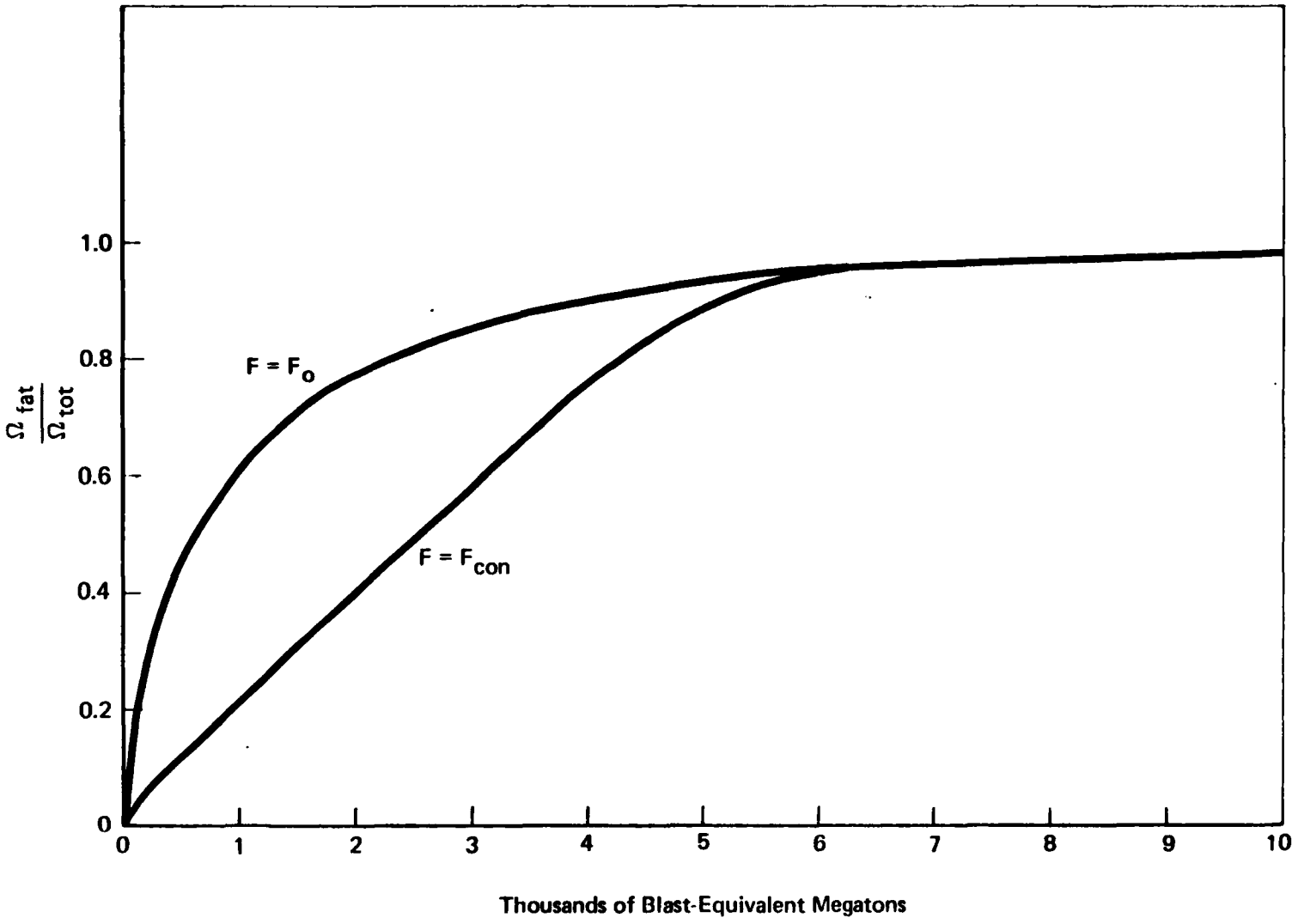

F_o and F_{con}. From one viewpoint (i.e., read "vertically"), Figure 20 indicates that for a given attack size, relocation can reduce fatalities appreciably; from another viewpoint (i.e., read "horizontally"), Figure 20 indicates that for a given fatality level, relocation can increase the required attack size by no more than a few thousand megatons. In Figure 21 (based on Equation 5), we illustrate the effect of increasing hardness without relocation, by plotting fatalities versus blast-equivalent megatons for prompt-effects hardnesses of 35 and 50 psi; Figure 21 presents both offense-conservative and defense-conservative estimates so that the relatively small difference between the two bounds may be recognized. The inevitable conclusion from these results is that to achieve moderate survivor fractions for attacks against population with several thousand blast-equivalent megatons, significant hardening is required, even with the most defense-optimistic assumptions about relocations which evacuate people to locations where at least some people already reside.

We now turn to exploring the influence of the delayed-effects hardness, $\langle\rho\rangle$. For combined (i.e., prompt-plus-delayed effects) casualties to exceed the (exclusively prompt-effects) casualties from an all-airburst attack, it is necessary--but by no means sufficient--that $\langle\rho\rangle$ be sufficiently small that the condition of Equation 25 is not satisfied. Even for such small values of $\langle\rho\rangle$, the excess $\hat{\Delta}$ of combined casualties (from a mix of surface and airbursts) over prompt casualties (from a pure airburst attack) is bounded via

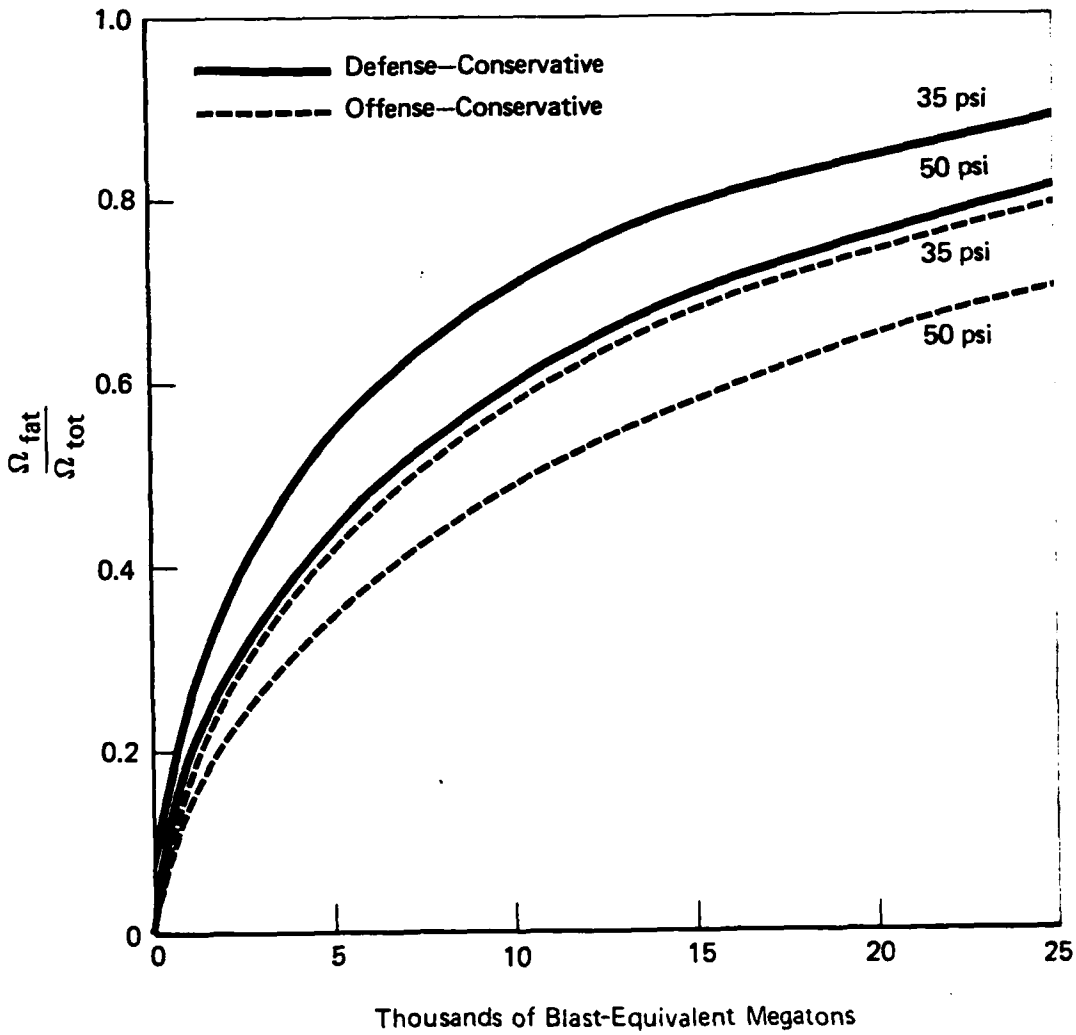

Figure 21. Fatalities vs Attack Size for Residential Population, 35 and 50 psi Hardness

$$\hat{\Delta} < F\left(\frac{\tau N s_{50,A}^{2}}{A^*}\,[1+\hat{\phi}]\right) - F\left(\frac{\tau N s_{50,A}^{2}}{A^*}\right) \qquad (49)$$

The value of delayed-effects hardness for which Equation 25 holds as an equality may naturally be called the breakeven value of protection factor, since this value gives $\hat{\phi} = 0$ in Equation 49, while larger values give $\hat{\phi} < 0$ and smaller values give $\hat{\phi} > 0$. In our discussion below, we restrict attention to values of $\langle\rho\rangle$ less than the breakeven value and to $F = F_o$ so that the results are applicable to residential population.

We begin by listing in Tables 10, 11, 12 (for $\Delta p_{s,50}$ = 5, 7, 10 psi, respectively) the values of the bound given by Equation 49 for Y = 1 Mt and various attack sizes and values of protection factor. In interpreting these tables, it is instructive to recall that

$$\frac{\tau N s_{50,A}^{2}}{A^*} = \frac{N}{\hat{N}} \quad \text{where } \hat{N} = \begin{Bmatrix} 1207 \\ 1808 \\ 2774 \end{Bmatrix} \text{ for } \Delta p_{s,50} = \begin{Bmatrix} 5 \\ 7 \\ 10 \end{Bmatrix} \text{ psi} \qquad (50)$$

for $A^* = 4 \times 10^4$ mi^2 and $\tau \simeq 2$. The general behavior shown in Tables 10 through 12 is that, for a fixed value of $\langle\rho\rangle$ the bound increases to a maximum and then decreases as the attack size increases. It should be noted that for $\langle\rho\rangle$ as small as half the breakeven value, the bound never exceeds some ten percent of the population. The location and magnitude of the maximum value of the bound

Table 10

Upper Bound on Incremental Fatalities - 5 psi Hardness

$\tau Ns_{50,A}^2/A^*$	$F(\tau Ns_{50,A}^2/A^*)$	$F(\tau Ns_{50}^2[1+\hat{\phi}]/A^*) - F(\tau Ns_{50,A}^2/A^*)$ for $\frac{<o>}{F/Y}$ =			
		6	10	30	50
0.05	0.1406	0.2358	0.1570	0.0431	0.0113
0.1	0.2090	0.3094	0.2121	0.0605	0.0160
0.2	0.3043	0.3729	0.2666	0.0806	0.0217
0.3	0.3740	0.3937	0.2905	0.0920	0.0250
0.4	0.4296	0.3966	0.3003	0.0990	0.0272
0.5	0.4760	0.3906	0.3024	0.1032	0.0287
0.6	0.5156	0.3800	0.2999	0.1057	0.0297
0.7	0.5501	0.3669	0.2946	0.1069	0.0303
0.8	0.5806	0.3528	0.2876	0.1072	0.0306
0.9	0.6077	0.3382	0.2795	0.1068	0.0307
1.0	0.6321	0.3236	0.2707	0.1059	0.0307
1.5	0.7250	0.2571	0.2257	0.0976	0.0293
2.0	0.7872	0.2047	0.1857	0.0870	0.0269

Table 11

Upper Bound on Incremental Fatalities - 7 psi Hardness

$\tau N s_{50,A}^2/A^*$	$F(\tau N s_{50,A}^2/A^*)$	$F(\tau N s_{50}^2[1+\hat{\phi}]/A^*) - F(\tau N s_{50,A}^2/A^*)$ for $\frac{<\rho>}{F/Y}$ =			
		10	30	50	80
0.05	0.1406	0.2183	0.0777	0.0365	0.0091
0.1	0.2090	0.2884	0.1080	0.0514	0.0129
0.2	0.3043	0.3509	0.1413	0.0686	0.0175
0.3	0.3740	0.3730	0.1591	0.0786	0.0202
0.4	0.4296	0.3779	0.1690	0.0847	0.0220
0.5	0.4760	0.3739	0.1743	0.0885	0.0232
0.6	0.5156	0.3652	0.1767	0.0908	0.0240
0.7	0.5501	0.3539	0.1770	0.0920	0.0245
0.8	0.5806	0.3413	0.1759	0.0924	0.0248
0.9	0.6077	0.3281	0.1739	0.0922	0.0249
1.0	0.6321	0.3147	0.1711	0.0916	0.0249
1.5	0.7250	0.2524	0.1524	0.0850	0.0238
2.0	0.7872	0.2021	0.1320	0.0762	0.0219

Table 12

Upper Bound on Incremental Fatalities - 10 psi Hardness

$\frac{\tau Ns_{50,A}^2}{A^*}$	$F\left(\frac{\tau Ns_{50,A}^2}{A^*}\right)$	$F(\tau Ns_{50,A}^2[1+\hat{\phi}]/A^*) - F(\tau Ns_{50,A}^2/A^*)$ for $\frac{<c>}{F/Y}$ =					
		10	30	50	80	100	150
0.05	0.1406	0.2950	0.1245	0.0715	0.0353	0.0217	0.0019
0.1	0.2090	0.3783	0.1701	0.0995	0.0497	0.0307	0.0027
0.2	0.3043	0.4415	0.2175	0.1307	0.0665	0.0413	0.0036
0.3	0.3740	0.4554	0.2401	0.1475	0.0761	0.0475	0.0042
0.4	0.4296	0.4503	0.2510	0.1570	0.0821	0.0515	0.0046
0.5	0.4760	0.4368	0.2552	0.1623	0.0858	0.0541	0.0049
0.6	0.5156	0.4196	0.2553	0.1648	0.0881	0.0557	0.0050
0.7	0.5501	0.4009	0.2528	0.1653	0.0892	0.0567	0.0051
0.8	0.5806	0.3818	0.2485	0.1646	0.0897	0.0572	0.0052
0.9	0.6077	0.3631	0.2431	0.1629	0.0895	0.0573	0.0052
1.0	0.6321	0.3449	0.2370	0.1606	0.0890	0.0571	0.0053
1.5	0.7250	0.2673	0.2025	0.1438	0.0826	0.0538	0.0051
2.0	0.7872	0.2082	0.1698	0.1252	0.0741	0.0489	0.0047

(as a function of attack size) are given by Equations 292, 295 and 296 of Ref. 1 and are listed in Table 13 for the cases considered in Tables 10, 11, 12. In Ref. 1, we solve the inverse problem of determining the value of $\langle\rho\rangle$ needed to guarantee that the maximum value of the bound never exceeds a specified value; the results are shown in Table 14 (reproduced from Ref. 1) and include the breakeven value $\hat{\psi}^*$ for $\langle\rho\rangle/(F/Y)$. These results clearly are concerned with bounding the <u>additive</u> effect of delayed casualties. A complementary and equally informative set of results concerns bounding the <u>multiplicative</u> effect of delayed casualties. We turn now to deriving these results.

From Equations 5, 6, 11 and 49, it follows that

$$\hat{\Delta} < \eta\, F\left(\frac{\tau N s_{50,\hat{A}}^{2}}{A^*}\right) \quad \text{if} \quad \frac{\langle\rho\rangle}{F/Y} > \frac{\hat{\psi}^*}{1+\delta\hat{\kappa}} \tag{51}$$

where

$$\delta = \left(\frac{\tau N s_{50,\hat{A}}^{2}}{A^*}\right)^{-1} \cdot \left\{F^{-1}\left[(1+\eta)F\left(\frac{\tau N s_{50,\hat{A}}^{2}}{A^*}\right)\right]\right\} - 1 \tag{52}$$

Equation 51 clearly is equivalent to the condition that the total combined-effects casualties from any mixed attack not exceed $(1+\eta)$ times the prompt-effects casualties from a pure airburst attack. For $F = F_0$, we write $\hat{\Delta} = \hat{\Delta}_0$ and illustrate Equation 51 for $\eta = 0.5$ and $\Delta p_{s,50} = 5, 7, 10$ psi; the results

Table 13

Location and Magnitude of Maximum Value of Upper Bound on Incremental Fatalities

$\Delta p_{s,50}$, psi	$\frac{\langle\rho\rangle}{F/Y}$	$\hat{\phi}$	Attack Size, $\frac{\tau N s_{50}^2}{A^*}$, Producing Maximum	Maximum Value of Upper Bound
5	6	5.0765	0.3728	0.3969
	10	2.8335	0.4872	0.3024
	30	0.5905	0.7885	0.1072
	50	0.1419	0.9354	0.0307
7	10	4.5219	0.3944	0.3779
	30	1.1631	0.6694	0.1771
	50	0.4913	0.8154	0.0924
	80	0.1135	0.9474	0.0249
10	10	7.2373	0.3106	0.4555
	30	2.0842	0.5508	0.2557
	50	1.0536	0.6884	0.1654
	80	0.4738	0.8205	0.0897
	100	0.2806	0.8823	0.0573
	150	0.0229	0.9887	0.0053

Table 14

Population-Weighted Protection Factor, $\frac{\langle\rho\rangle}{(F/Y)}$, to Guarantee that $\hat{\Delta} < 0$ and $\hat{\Delta}_o < \Delta_{max}$

$\Delta p_{s,50}$, psi	$\hat{\psi}$	$\hat{\psi}*(1+\hat{\kappa}\ \hat{x})^{-1}$ for Δ_{max} =			
		1/20	1/10	1/6	1/4
1	9.3	6.4	4.6	3.1	1.9
2	20.7	14.3	10.4	7.0	4.4
3	33.7	23.3	16.8	11.3	7.2
4	47.9	33.0	23.9	16.1	10.1
5	63.3	43.6	31.4	21.1	13.3
6	79.9	54.7	39.3	26.3	16.6
7	97.5	66.5	47.6	31.8	20.0
8	116	78.9	56.3	37.6	23.5
9	136	91.9	65.4	43.4	27.2
10	160	105	74.7	49.6	31.0
15	277	181	126	82.8	51.2
20	427	270	185	120	73.4
25	608	373	251	160	97.3
30	827	489	324	204	123
35	1090	621	404	251	150
40	1410	769	491	301	178
45	1790	934	585	354	207
50	2260	1120	686	410	238
55	2840	1320	795	469	270
60	3570	1560	912	530	303
65	4510	1810	1040	595	337
70	5740	2100	1170	663	372
75	7420	2420	1320	734	409
80	9840	2790	1470	808	446
90	20,100	3660	1810	965	525
100	87,700	4810	2210	1140	607

are summarized in Table 15 and display the bound of Equation 51 as a function of attack size. It is apparent that, for fixed values of η and $\Delta p_{s,50}$, the required protection factor decreases steadily with increasing attack size. For $F = F_o$, it is readily seen that

$$\delta > (1+\eta)^{1/\lambda} - 1 \tag{53}$$

where the right-hand side of Equation 53 is the limit of Equation 52 as attack size becomes vanishingly small. It follows immediately that

$$\hat{\Delta}_o < \eta F\left(\frac{\tau N s_{50,A}^2}{A^*}\right) \quad \text{if} \quad \frac{\langle\rho\rangle}{F/Y} > \frac{\hat{\psi}^*}{1+[(1+\eta)^{1/\lambda} - 1]\hat{\kappa}} \tag{54}$$

In Table 16 we list this bound on protection factor for several values of $\Delta p_{s,50}$ and η. If the protection factor satisfies Equation 54, it clearly satisfies Equation 51 also; the converse, of course, is not true, as may be seen by comparing Tables 15 and 16.

From the results presented in Tables 10 through 16, we see that the breakeven values of protection factor are modest and, moreover, that even less-than-breakeven values typically do not materially alter the outcome, i.e., maximum number of fatalities. Consequently, for attacks against population, the influence of delayed-effects hardness is generally weak, compared

Table 15

Population-Weighted Protection Factor, $\frac{\langle \rho \rangle}{F/Y}$, to Guarantee that $\hat{\Delta}_o < 0.5\ F(\tau Ns_{50,A}^2/A^*)$ for Various Attack Sizes and Blast Hardnesses

$\tau Ns_{50,A}^2/A^*$	δ	$\frac{\hat{\psi}^*}{1+\delta\hat{\kappa}}$ for $\Delta p_{s,50}$ =		
		5 psi	7 psi	10 psi
0.05	1.0322	21.5	32.5	50.7
0.1	1.1177	20.4	30.8	48.0
0.2	1.2787	18.6	28.0	43.6
0.3	1.4476	17.0	25.6	39.8
0.4	1.6362	15.5	23.4	36.3
0.5	1.8556	14.1	21.2	32.9
0.6	2.1204	12.7	19.1	29.6
0.7	2.4536	11.3	17.0	26.2
0.8	2.8965	9.8	14.8	22.8
0.9	3.5352	8.3	12.4	19.2
1.0	4.5986	6.6	9.9	15.2
1.1	7.1400	4.4	6.6	10.1
1.15	12.8336	2.5	3.8	5.8

Table 16

Population-Weighted Protection Factor, $\frac{\langle \rho \rangle}{F/Y}$, to Guarantee that $\hat{\Delta}_o < \eta F(\tau N s_{50,A}^2/A^*)$

$\Delta p_{s,50}$ (psi)	$\frac{\hat{v}^*}{1+[(1+\eta)\frac{1}{\lambda} -1]\hat{\kappa}}$ for η =						
	0	0.1	0.3	0.5	0.7	0.9	1.0
1	9.3	7.1	4.7	3.4	2.6	2.1	1.9
2	20.7	15.9	10.6	7.8	6.0	4.9	4.4
3	33.7	25.9	17.2	12.6	9.8	7.9	7.2
4	47.9	36.8	24.4	17.9	13.8	11.2	10.1
5	63.3	48.5	32.1	23.5	18.2	14.6	13.3
6	79.9	60.9	40.2	29.3	22.7	18.3	16.6
7	97.5	74.1	48.8	35.5	27.4	22.0	20.0
8	116	88.0	57.7	41.9	32.3	26.0	23.5
9	136	103	67.0	48.5	37.4	30.0	27.2
10	157	118	76.6	55.4	42.6	34.2	31.0
15	278	204	130	92.7	70.9	56.6	51.2
20	427	307	190	135	102	81.2	73.4
25	608	426	258	181	136	108	97.3
30	827	564	334	231	173	136	123
35	1090	721	416	284	212	166	150
40	1410	901	506	342	253	198	178
45	1790	1110	604	403	297	231	207
50	2260	1340	709	468	342	266	238
55	2850	1600	823	537	390	302	270
60	3580	1900	945	610	440	339	303
65	4520	2250	1080	686	492	378	337
70	5750	2640	1220	766	547	418	372
75	7440	3100	1370	851	603	460	409
80	9870	3630	1530	939	662	503	446
90	20,300	4980	1890	1130	785	592	525
100	89,900	6920	2310	1340	917	687	607

to the influence of prompt-effects hardness and dispersion. For populations with protection factor very small compared to the breakeven value, this conclusion has not been demonstrated above. If, for some reason, it is necessary to consider such populations, tighter bounds than those employed above may yet enable the conclusion to be extended even to many such populations. In deriving the bounds used above, we have significantly overestimated both the size of the fallout region and the population contained therein. Both these overestimates can be tightened up, e.g., by restricting the number of effectively collocated bursts to be less than a small fixed maximum, by narrowing the range of admissible meteorological conditions, by accounting for overlap between prompt and delayed effects, by accounting for extensive unpopulated areas.

The positive interpretation of our results concerning delayed-effects hardness is that--precisely because the breakeven values of protection factor are modest--realizable, finite levels of fallout shielding provide as much guaranteed protection as any level of shielding can provide. Consequently, efforts to provide the population with this assured protection have demonstrable payoff.

The bounds derived above for protection factor depend upon, inter alia, "universal" isodose contours and the area contained therein (cf. Ref. 1). In Appendix B, we present numerical details, omitted from Ref. 1, to illustrate more comprehensively the behavior of the isodose contours.

3. CONCLUSIONS AND RECOMMENDATIONS

In this section, we summarize the major conclusions which have emerged from this investigation and offer the corollary recommendations for future action.

3.1 Conclusions

The principal conclusions from the results presented here are listed below.

1. The feasibility of interrelating analytically the major ingredients of damage/casualty prediction has been demonstrated by deriving tractable, explicit analytic representations of the interplay among the characteristics of the attack, targets, environment and outcome.

2. Our approach for determining the effective blast protection of a population with mixed, non-uniform protection produces stable, consistent values of protection hardness and accurate estimates of casualties.

3. Relocation schemes which evacuate a region's population to locations where at least some people already reside have been characterized abstractly and analyzed parametrically; in particular, the conditions for, and consequences of, self-contained regional relocation have been determined.

4. It is highly unlikely that any realistic approach could relocate the bulk of the nation's population at population density less than 1,000 to 1,500 people/mi^2, i.e., some 2 to 3 times the population density corresponding to spreading the entire population uniformly over the entire populated area.

5. To achieve moderate survivor fractions for attacks against population with several thousand blast-equivalent megatons, significant blast hardening is required, even with the most defense-optimistic assumptions about relocation.

6. For attacks against population, the influence of delayed-effects hardness is generally weak, compared to the influence of prompt-effects hardness and dispersion.

3.2 Recommendations

In view of the results and conclusions presented above, we recommend that

1. the demographics of residential population be analyzed to

   a) explore the validity of the apparent universality of normalized, rank-ordered population distribution for different geographic regions,

   b) provide a basis for interpreting the rank-ordered population distribution in other commonly used formats (e.g., in terms of political subdivisions)

2. the general analytic approach and results be extended, refined, and applied, e.g., by considering

   a) attacks more general than attacks against population,

   b) tighter bounds on combined-effects casualties,

   c) specific candidate relocation schemes.

APPENDIX A

RANK-ORDERED POPULATION DISTRIBUTION FOR SELF-CONTAINED RELOCATION WITH COMPLETE HOSTING

In this Appendix, we complete the characterization--discussed in Section 2.3 of the text--of the rank-ordered population distribution G for self-contained (r=S) relocation with complete hosting and no buffer region. The previous discussion has shown that G consists of four portions, with progressively smaller post-relocation population densities in each portion. We follow the notation introduced in the text and prescribe below the end-points of each of these four portions, i.e., we state the incremental area and incremental population of each portion. The behavior between end-points is readily inferred from the definition of the relocation and from the previously discussed properties of $F = F_o$ and of the critical hosting parameters. The cumulative distribution defined by the four portions is simply G itself.

The initial portion of G consists of that portion of the evacuation region which, even after relocation, has population density greater than ω^*. The size of this portion is clearly given by $A/A^* = a_1$, where

$$(1-\gamma)F'(a_1) = F'(\hat{a}) \qquad (1)$$

Therefore this first portion of G has incremental area

$$\Delta(A/A^*) = a_1 \tag{2}$$

and incremental population

$$\Delta G = (1-\gamma)F(a_1) \tag{3}$$

The next portion of G consists of that part of the host region which has constant population density ω^*. This portion has incremental area

$$\Delta(A/A^*) = \tilde{a}-\hat{\hat{a}} \tag{4}$$

and incremental population

$$\Delta G = F'(\hat{\hat{a}})[\tilde{a}-\hat{\hat{a}}] \tag{5}$$

We have seen that, after relocation, the smallest population density is $(1-\gamma)\omega^*$ in the evacuation region and is $\hat{K}^*F'(10)\Omega_{tot}/A^*$ in the host region. Therefore, we have from Equation 48 of the text that the least densely populated (post-relocation) cells are in the host region if

$$(1-\gamma)F'(\tilde{a}) > F'(10) \tag{6}$$

AD-A085 170 LA JOLLA INST CA F/G 15/6
DEMOGRAPHICS AND CASUALTY PREDICTION/ANALYSIS.(U)
FEB 80 J J SHEA DCPA01-79-C-0244
UNCLASSIFIED LJI-R-80-060 NL

END
DATE FILMED
7-80
DTIC

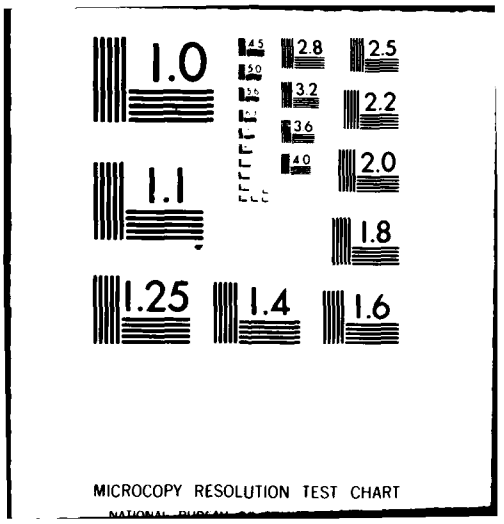
1.0
1.1
1.25
1.4
1.6
1.8
2.0
2.2
2.5
2.8
3.2
3.6
4.0
4.5
5.0
MICROCOPY RESOLUTION TEST CHART

and in the evacuation region if the reverse inequality holds. For a fixed γ, Equation 6 is satisfied for sufficiently small $\tilde{a}$ and hence for sufficiently small $\hat{K}^*$.

If Equation 6 is satisfied, then the portion of G following the constant-population-density portion consists of the balance of the evacuation region, plus that portion of the host region wherein the post-relocation population density exceeds $(1-\gamma)\omega^*$. The incremental area of this portion is

$$\Delta(A/A^*) = \hat{\tilde{a}} - a_1 + a_3 - \tilde{a} \tag{7}$$

and the incremental population is

$$\Delta G = (1-\gamma)[F(\hat{\tilde{a}}) - F(a_1)] + \hat{K}^*[F(a_3) - F(\tilde{a})] \tag{8}$$

where the parameter a_3 is given (via Equation 48 of the text) by

$$F'(a_3) = (1-\gamma)F'(\tilde{a}) \tag{9}$$

and thus defines the host-region location where the post-relocation population density is $(1-\gamma)\omega^*$.

If Equation 6 is satisfied, then the remaining portion of G consists of the balance of the host region and has incremental area

$$\Delta(A/A^*) = 10-a_3 \tag{10}$$

and incremental population

$$\Delta G = \hat{K}^*[F(10)-F(a_3)] \tag{11}$$

If Equation 6 is not satisfied (i.e., if $\tilde{a}$ or $\hat{K}^*$ is sufficiently large), then the portion of G following the constant-population-density portion consists of the balance of the host region plus that portion of the evacuation region wherein the post-relocation population density exceeds $\hat{K}^*F'(10)\Omega_{tot}/A^*$. The incremental area of this portion is

$$\Delta(A/A^*) = a_2-a_1 + 10-\tilde{a} \tag{12}$$

and the incremental population is

$$\Delta G = (1-\gamma)[F(a_2)-F(a_1)] + \hat{K}^*[F(10)-F(\tilde{a})] \tag{13}$$

where the parameter a_2 is given by

$$(1-\gamma)F'(a_2) = \hat{K}^*F'(10) \tag{14}$$

and thus defines the evacuation-region location where the post-relocation population density is $\hat{K}^*F'(10)\Omega_{tot}/A^*$.

If Equation 6 is not satisfied, then the remaining portion of G consists of the balance of the evacuation region and has incremental area

$$\Delta(A/A^*) = \hat{\tilde{a}} - a_2 \tag{15}$$

and incremental population

$$\Delta G = (1-\gamma)[F(\hat{\tilde{a}}) - F(a_2)] \tag{16}$$

In sum, then, the distribution G has the cumulative behavior determined by the four constituent portions. Thus the first portion (from Equation 2 for A and from Equation 3 for G) ends with

$$A/A^* = a_1 \qquad G = (1-\gamma)F(a_1) \tag{17}$$

while the second portion (from Equations 2 and 4 for A and from Equations 3 and 5 for G) ends with

$$A/A^* = a_1 + \tilde{a} - \hat{a} \qquad G = (1-\gamma)F(a_1) + F'(\hat{a})[\tilde{a} - \hat{a}] \tag{18}$$

If $\hat{K}^*$ is sufficiently small that Equation 6 is satisfied, then the third portion (from Equations 2, 4 and 7 for A and from Equations 3, 5 and 8 for G) ends with

$$A/A^* = a_3 \qquad G = (1-\gamma)F(\hat{\hat{a}}) + F'(\hat{\hat{a}})[\tilde{\tilde{a}}-\hat{\hat{a}}]+\hat{K}^*[F(a_3)-F(\tilde{\tilde{a}})] \tag{19}$$

while the fourth portion (from Equations 2, 4, 7 and 10 for A and from Equations 3, 5, 8 and 11 for G) ends with

$$A/A^* = 10 \qquad G = (1-\gamma)F(\hat{\hat{a}}) + F'(\hat{\hat{a}})[\tilde{\tilde{a}}-\hat{\hat{a}}] + \hat{K}^*[F(10)-F(\tilde{\tilde{a}})] \tag{20}$$

From Equations 41 and 43 of the text, we see that for the conditions considered here (i.e., $\Gamma=S$, $\hat{\hat{A}}=\hat{A}$) the expression for G(10) given by Equation 20 is in fact F(10), as it should be.

If $\hat{K}^*$ is sufficiently large that Equation 6 is not satisfied, then the third portion (from Equations 2, 4 and 12 for A and from Equations 3, 5 and 13 for G) ends with

$$A/A^* = 10-(\hat{\hat{a}}-a_2) \qquad G = (1-\gamma)F(a_2) + F'(\hat{\hat{a}})[\tilde{\tilde{a}}-\hat{\hat{a}}] + \hat{K}^*[F(10)-F(\tilde{\tilde{a}})] \tag{21}$$

while the fourth portion (from Equations 2, 4, 12 and 15 for A and from Equations 3, 5, 13 and 16 for G) ends with

$$A/A^* = 10 \qquad G = (1-\gamma)F(\hat{\hat{a}}) + F'(\hat{\hat{a}})[\tilde{\tilde{a}}-\hat{\hat{a}}] + \hat{K}^*[F(10)-F(\tilde{\tilde{a}})] \tag{22}$$

Af before, G(10) as given by Equation 22 is, in fact, F(10).

For $\gamma = 1$ (i.e., for 100 percent evacuation) the distribution G is degenerate and is given simply as

$$G(\frac{A}{A^*}) = \begin{cases} [F'(\hat{\hat{a}})]\,\frac{A}{A^*} & 0 < \frac{A}{A^*} < \tilde{\hat{a}} - \hat{\hat{a}} \\ F'(\hat{\hat{a}})[\tilde{\hat{a}} - \hat{\hat{a}}] + \hat{K}^*[F(\hat{\hat{a}} + \frac{A}{A^*}) - F(\tilde{\hat{a}})] & \hat{\hat{a}} - \hat{\hat{a}} < \frac{A}{A^*} < 10 - \hat{\hat{a}} \end{cases} \tag{23}$$

where the parameters $\hat{\hat{a}}$, $\tilde{\hat{a}}$, etc. are tabulated in Table 8 as a function of $\hat{K}^*$.

We now illustrate the behavior of G for less than complete (γ=1) evacuation. Specifically, we consider the case $\gamma = 0.8$, corresponding to 80 percent evacuation. For $\gamma = 0.8$, Equation 6 is satisfied for $\tilde{\hat{a}}$ less than 5.3777 and hence, from Table 9, for $\hat{K}^*$ less than a value intermediate between 7 and 8. In Table A.1, we list the values of a_1, a_2, a_3 determined, for $\gamma = 0.8$, from Equations 1, 14, 9 respectively. These values together with the values tabulated for $\hat{\hat{a}}$, $\tilde{\hat{a}}$, etc. in Table 9, suffice to determine the distribution G. In Table A.2 we summarize, for $\gamma = 0.8$ and various values of $\hat{K}^*$, the location of, and the magnitude of G at, the end of the four constituent regions.

Table A.1

The Parameters a_1, a_2, a_3 for 80 Percent Evacuation

$\hat{K}^*$	$\tilde{a}$	a_1	$F(a_1)$	a_2	$F(a_2)$	a_3	$F(a_3)$
2	1.1508	0.0321	0.1082			3.6789	0.8969
3	2.3153	0.0850	0.1907			5.6484	0.9490
4	3.2408	0.1337	0.2453			7.0410	0.9673
5	3.9967	0.1747	0.2833			8.1188	0.9763
6	4.6325	0.2088	0.3111			8.9966	0.9815
7	5.1795	0.2372	0.3323			9.7354	0.9849
8	5.6580	0.2610	0.3489	1.4846	0.7227		
9	6.0825	0.2811	0.3621	1.3404	0.6996		
10	6.4632	0.2981	0.3728	1.2185	0.6778		
15	7.9224	0.3521	0.4044	0.8122	0.5841		
20	8.9333	0.3761	0.4173	0.5833	0.5094		

Table A.2

The Distribution G for 80 Percent Evacuation

$\hat{K}^*$	A/A*	G(A/A*)	Δ(A/A*)	ΔG
2	0.0321	0.0217	0.0321	0.0217
	0.6421	0.2664	0.6100	0.2447
	3.6789	0.8078	3.0368	0.5414
	10.0	0.9860	6.3211	0.1781
3	0.0850	0.0381	0.0850	0.0381
	1.4887	0.3944	1.4037	0.3563
	5.6484	0.8751	4.1597	0.4807
	10.0	0.9860	4.3516	0.1108
4	0.1337	0.0491	0.1337	0.0491
	2.2217	0.4671	2.0880	0.4180
	7.0410	0.9112	4.8193	0.4441
	10.0	0.9860	2.9590	0.0747
5	0.1747	0.0567	0.1747	0.0567
	2.8478	0.5171	2.6731	0.4604
	8.1188	0.9376	5.2710	0.4205
	10.0	0.9860	1.8812	0.0485
6	0.2088	0.0622	0.2088	0.0622
	3.3897	0.5551	3.1809	0.4929
	8.9966	0.9593	5.6069	0.4042
	10.0	0.9860	1.0034	0.0267
7	0.2372	0.0665	0.2372	0.0665
	3.8656	0.5863	3.6284	0.5198
	9.7354	0.9787	5.8698	0.3924
	10.0	0.9860	0.2646	0.0073

Table A.2, continued

$\hat{K}^*$	A/A*	G(A/A*)	Δ(A/A*)	ΔG
8	0.2610	0.0698	0.2610	0.0698
	4.2886	0.6129	4.0276	0.5431
	9.8542	0.9818	5.5656	0.3689
	10.0	0.9860	0.1458	0.0042
9	0.2811	0.0724	0.2811	0.0724
	4.6688	0.6364	4.3877	0.5640
	9.6456	0.9755	4.9768	0.3391
	10.0	0.9860	0.3544	0.0105
10	0.2981	0.0746	0.2981	0.0746
	5.0135	0.6577	4.7154	0.5831
	9.4707	0.9698	4.4572	0.3121
	10.0	0.9860	0.5293	0.0162
15	0.3521	0.0809	0.3521	0.0809
	6.3665	0.7451	6.0144	0.6642
	8.9042	0.9474	2.5377	0.2023
	10.0	0.9860	1.0958	0.0387
20	0.3761	0.0835	0.3761	0.0835
	7.3337	0.8171	6.9576	0.7336
	8.6076	0.9310	1.2739	0.1139
	10.0	0.9860	1.3924	0.0551

APPENDIX B

UNIVERSAL ISODOSE CONTOURS

In this Appendix, we present numerical details, omitted from Ref. 1, to illustrate more comprehensively the behavior of "universal" isodose contours as functions of downwind location, x, and crosswind location, y.

We have shown in Ref. 1 that, in the far-field approximation to WSEG-10 fallout phenomenology, it is possible to characterize each isodose contour in purely geometric terms by specifying the distant location, $\hat{x}$, at which the isodose contour crosses the downwind axis. The crosswind extent, $y_{isodose}$, of the isodose contour is given in dimensionless form as

$$v \equiv \frac{y_{isodose}}{(\sigma_H S_c/W)\hat{x}} = 2^{1/2} \frac{x}{\hat{x}} \left\langle \frac{\hat{x}}{WT} \left(1 - \frac{x}{\hat{x}}\right) + c \log\left(\frac{x}{\hat{x}}\right)^{-1} \right\rangle^{1/2} \qquad (1)$$

where

$$c = 1.382 \qquad (2)$$

Equation 1 presents the isodose contour's dimensionless crosswind extent, v, as a function of the parameter $\hat{x}/WT$ and of the normalized location, $x/\hat{x}$. Table B.1 lists v as a function of $x/\hat{x}$ for several values of $\hat{x}/WT$. For some of these values of $\hat{x}/WT$, Figure B.1 (from Ref. 1) presents the corresponding plot of v as a function of $x/\hat{x}$.

Table B.1

Normalized Isodose Contours for Several Values of $\hat{x}/WT$ and Normalized Distance

$\frac{x}{\hat{x}}$	v, for $\hat{x}/WT$ =					
	0.1	0.2	0.4	0.6	0.8	1.0
0.99	0.1708	0.1765	0.1873	0.1975	0.2071	0.2164
0.95	0.3701	0.3821	0.4050	0.4267	0.4474	0.4671
0.9	0.5021	0.5180	0.5483	0.5771	0.6046	0.6308
0.8	0.6483	0.6678	0.7051	0.7405	0.7743	0.8067
0.7	0.7159	0.7361	0.7750	0.8121	0.8475	0.8815
0.6	0.7329	0.7523	0.7896	0.8253	0.8595	0.8924
0.5	0.7099	0.7273	0.7609	0.7931	0.8240	0.8538
0.4	0.6515	0.6660	0.6943	0.7214	0.7475	0.7728
0.3	0.5587	0.5698	0.5915	0.6125	0.6327	0.6523
0.2	0.4293	0.4367	0.4512	0.4651	0.4787	0.4919
0.1	0.2558	0.2593	0.2662	0.2728	0.2794	0.2857
0.05	0.1455	0.1471	0.1503	0.1535	0.1565	0.1595
0.01	0.0360	0.0362	0.0368	0.0373	0.0378	0.0384

Table B.1, continued

$\frac{x}{\hat{x}}$	v, for $\hat{x}/WT$ =					
	1.0	2.0	4.0	6.0	8.0	10.0
0.99	0.2164	0.2577	0.3250	0.3806	0.4290	0.4725
0.95	0.4671	0.5554	0.6993	0.8182	0.9219	1.0151
0.9	0.6308	0.7483	0.9402	1.0990	1.2377	1.3623
0.8	0.8067	0.9522	1.1911	1.3895	1.5629	1.7189
0.7	0.8815	1.0349	1.2880	1.4990	1.6838	1.8502
0.6	0.8924	1.0413	1.2885	1.4954	1.6770	1.8407
0.5	0.8538	0.9894	1.2161	1.4068	1.5745	1.7260
0.4	0.7728	0.8884	1.0832	1.2479	1.3933	1.5249
0.3	0.6523	0.7426	0.8964	1.0274	1.1435	1.2488
0.2	0.4919	0.5531	0.6587	0.7496	0.8306	0.9044
0.1	0.2587	0.3157	0.3683	0.4143	0.4557	0.4936
0.05	0.1595	0.1738	0.1992	0.2218	0.2423	0.2612
0.01	0.0384	0.0409	0.0454	0.0496	0.0534	0.0570

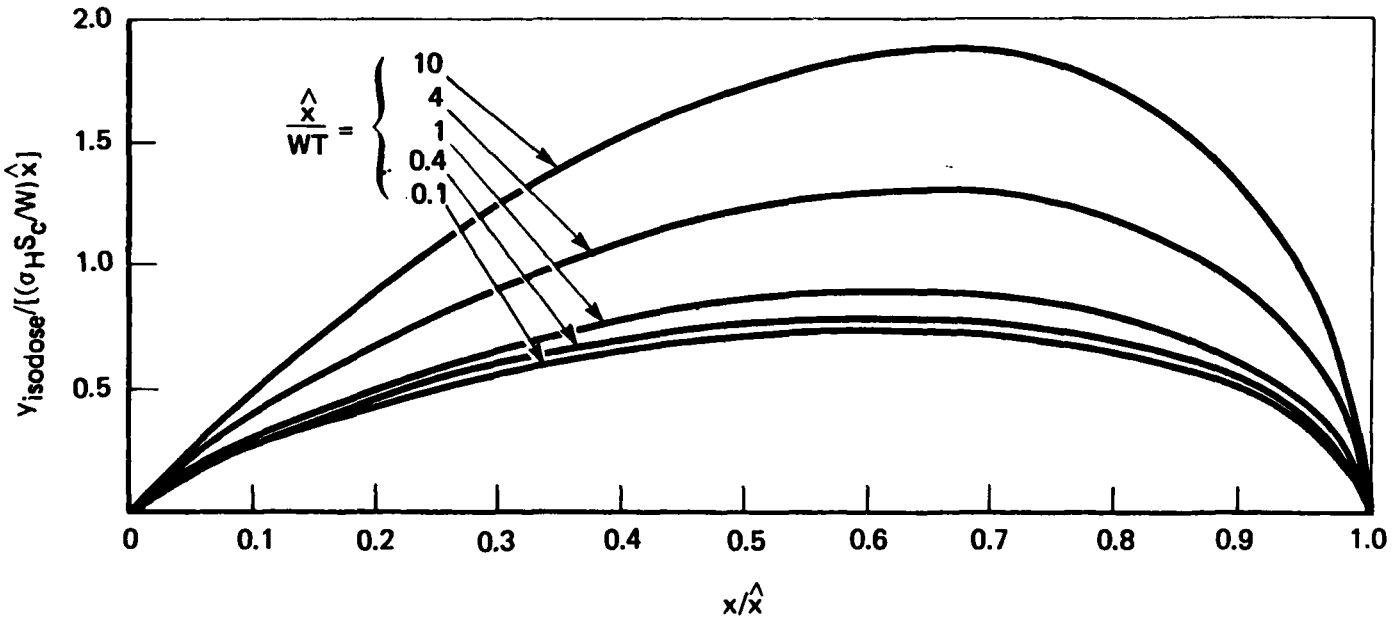

Figure B.1 Normalized Isodose Contours, for Various Values of $\hat{x}/WT$

For a given value of $\hat{x}/WT$, v increases from 0 to a maximum, v_{max}, and then decreases to 0 as $x/\hat{x}$ increases from 0 to u* (i.e., the value of $x/\hat{x}$ yielding v_{max}) to 1. The downwind location, $x/\hat{x} = u^*$, and magnitude, v_{max}, of the maximum crosswind extent of the universal isodose contour are given by

$$\frac{\hat{x}}{WT} = \frac{(c/3)(1+2 \log u^*)}{\frac{2}{3} - u^*} \tag{3}$$

$$v_{max} = u^* \left(c + \frac{\hat{x}}{WT} u^* \right)^{1/2} \tag{4}$$

It follows immediately from Equations 3 and 4 that as $\hat{x}/WT$ increases, then u* increases from $e^{-1/2} = 0.6065$ to $2/3 = 0.6667$ and v_{max} increases monotonically and unboundedly from $(c/e)^{1/2} = 0.7130$. In Table B.2, we list u* and v_{max} for several values of $\hat{x}/WT$.

To prepare isodose contours in the more conventional format (i.e., as loci of points in the x-y plane), it suffices to recognize that

$$\frac{x}{WT} = \frac{\hat{x}}{WT} \frac{x}{\hat{x}} \tag{5}$$

$$\frac{y_{isodose}}{WT} = (\sigma_H S_c / W) \frac{\hat{x}}{WT} v \tag{6}$$

Table B.3 lists values of $y_{isodose}/WT$ as a function of x/WT for $\sigma_H S_c/W = 0.1$ and for several values of $\hat{x}/WT$. Figures B.2 and B.3 (from Ref. 1) present the

Table B.2

Downwind Location and Magnitude of Maximum Crosswind Extent of Universal Isodose Contour

$\frac{\hat{x}}{WT}$	u*	v_{max}
10^{-2}	0.6069	0.7151
0.1	0.6103	0.7331
0.2	0.6136	0.7526
0.4	0.6192	0.7904
0.6	0.6237	0.8266
0.8	0.6275	0.8613
1.0	0.6307	0.8947
2.0	0.6411	1.0465
4.0	0.6505	1.2985
6.0	0.6549	1.5093
8.0	0.6574	1.6941
10.0	0.6590	1.8607
10^{2}	0.6658	5.4889
10^{3}	0.6666	17.2277

Table B.3

Universal Isodose Contours for $\sigma_H S_c/W=0.1$ and Several Values of $\hat{x}/WT$

$\hat{x}/WT=0.1$		$\hat{x}/WT=0.2$		$\hat{x}/WT=0.4$		$\hat{x}/WT=0.6$	
x/WT	y/WT	x/WT	y/WT	x/WT	y/WT	x/WT	y/WT
0.099	0.0017	0.198	0.0035	0.396	0.0075	0.594	0.0118
0.095	0.0037	0.19	0.0076	0.38	0.0162	0.57	0.0256
0.09	0.0050	0.18	0.0104	0.36	0.0219	0.54	0.0346
0.08	0.0065	0.16	0.0134	0.32	0.0282	0.48	0.0444
0.07	0.0072	0.14	0.0147	0.28	0.0310	0.42	0.0487
0.06	0.0073	0.12	0.0150	0.24	0.0316	0.36	0.0495
0.05	0.0071	0.10	0.0145	0.20	0.0304	0.30	0.0476
0.04	0.0065	0.08	0.0133	0.16	0.0278	0.24	0.0433
0.03	0.0056	0.06	0.0114	0.12	0.0237	0.18	0.0367
0.02	0.0043	0.04	0.0087	0.08	0.0180	0.12	0.0279
0.01	0.0026	0.02	0.0052	0.04	0.0106	0.06	0.0164
0.005	0.0015	0.01	0.0029	0.02	0.0060	0.03	0.0092
0.001	0.0004	0.002	0.0007	0.004	0.0015	0.006	0.0022

Table B.3, continued

$\hat{x}$/WT=0.8		$\hat{x}$/WT=1.0		$\hat{x}$/WT=2.0		$\hat{x}$/WT=4.0	
x/WT	y/WT	x/WT	y/WT	x/WT	y/WT	x/WT	y/WT
0.792	0.0166	0.99	0.0216	1.98	0.0515	3.96	0.1300
0.76	0.0358	0.95	0.0467	1.90	0.1111	3.80	0.2797
0.72	0.0484	0.9	0.0631	1.80	0.1497	3.60	0.3761
0.64	0.0619	0.8	0.0807	1.60	0.1904	3.20	0.4764
0.56	0.0678	0.7	0.0882	1.40	0.2070	2.80	0.5152
0.48	0.0688	0.6	0.0892	1.20	0.2083	2.40	0.5154
0.40	0.0659	0.5	0.0854	1.00	0.1979	2.00	0.4865
0.32	0.0598	0.4	0.0773	0.80	0.1777	1.60	0.4333
0.24	0.0506	0.3	0.0652	0.60	0.1485	1.20	0.3586
0.16	0.0383	0.2	0.0492	0.40	0.1106	0.80	0.2635
0.08	0.0223	0.1	0.0286	0.20	0.0631	0.40	0.1473
0.04	0.0125	0.05	0.0160	0.10	0.0348	0.20	0.0797
0.008	0.0030	0.01	0.0038	0.02	0.0082	0.04	0.0182

Table B.3, concluded

$\hat{x}$/WT=6.0		$\hat{x}$/WT=8.0		$\hat{x}$/WT=10.0	
x/WT	y/WT	x/WT	y/WT	x/WT	y/WT
5.94	0.2283	7.92	0.3432	9.9	0.4725
5.70	0.4909	7.60	0.7375	9.5	1.0151
5.40	0.6594	7.20	0.9902	9.0	1.3623
4.80	0.8337	6.40	1.2503	8.0	1.7189
4.20	0.8994	5.60	1.3470	7.0	1.8502
3.60	0.8973	4.80	1.3416	6.0	1.8407
3.00	0.8441	4.00	1.2596	5.0	1.7260
2.40	0.7487	3.20	1.1146	4.0	1.5249
1.80	0.6164	2.40	0.9148	3.0	1.2488
1.20	0.4498	1.60	0.6645	2.0	0.9044
0.60	0.2486	0.80	0.3645	1.0	0.4936
0.30	0.1331	0.40	0.1938	0.5	0.2612
0.06	0.0298	0.08	0.0428	0.1	0.0570

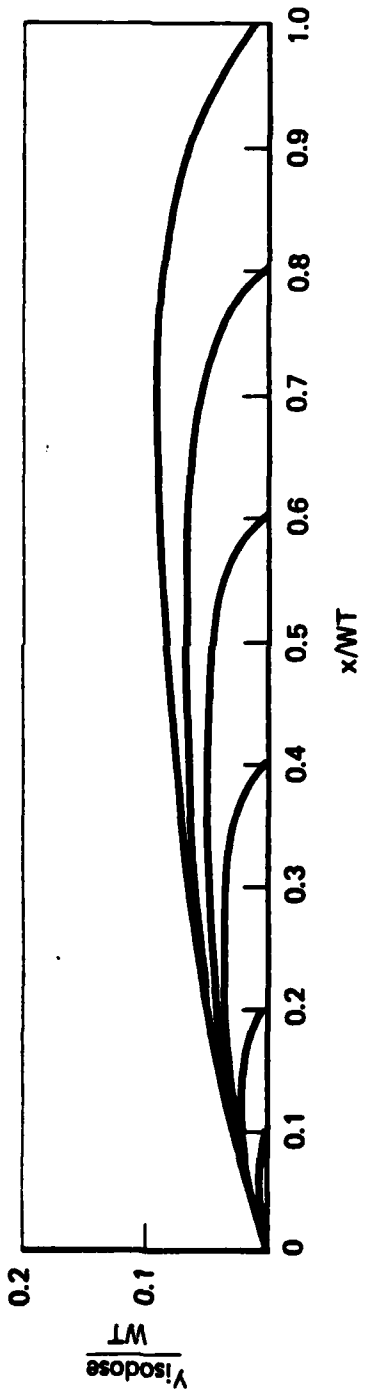

Figure B.2 Isodose Contours for $\sigma_H S_c/W = 0.1$ and $\hat{x}/WT \leq 1$

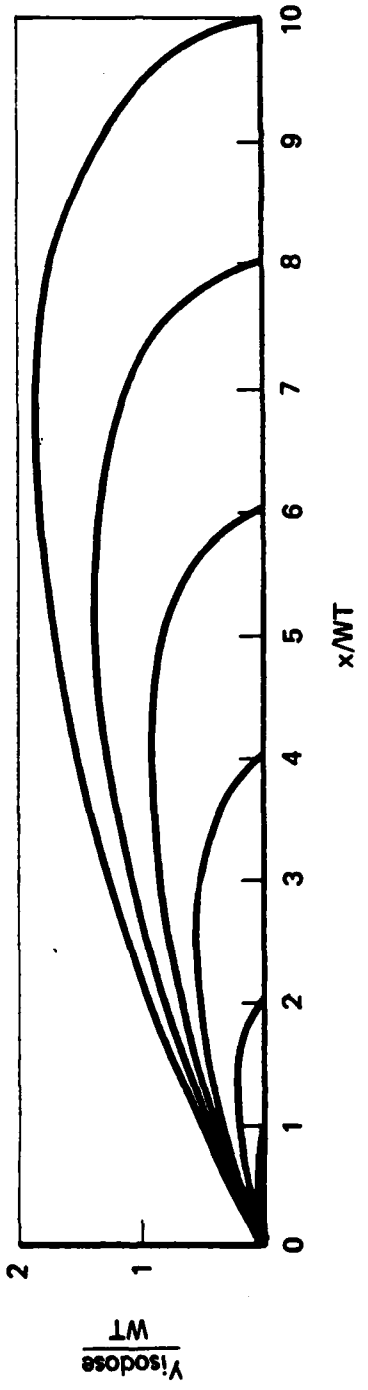

Figure B.3 Isodose Contours for $\sigma_H S_c/W = 0.1$ and $\hat{x}/WT \geq 1$

corresponding plots. To obtain results for any other value of $\sigma_H S_c/W$, it suffices to multiply the scale of the crosswind axis by $(\sigma_H S_c/W)/0.1$. It is clear that the downwind location and magnitude of the maximum crosswind extent of each isodose contour are given by

$$\frac{x}{WT} = \frac{\hat{x}}{WT} u^* \tag{7}$$

$$\frac{y}{WT} = (\sigma_H S_c/W) \frac{\hat{x}}{WT} v_{max} \tag{8}$$

REFERENCES

1. J.J. Shea, "Damage/Casualty Prediction and Analysis", LJI-TN-79-032, DCPA Work Unit 4111B, July, 1979.

2. L.A. Schmidt, "Methodology of Fallout-Risk Assessment", IDA P-1065, January 1975.

3. G.N. Sisson, D.W. Bensen, "Protection of Risk Area Residents and Key Workers From the Effects of Nuclear Weapons", DCPA REP-3, January, 1977.

DISTRIBUTION

	No. of Copies
Federal Emergency Management Agency Mitigation and Research ATTN: Administrative Officer Washington, D. C. 20472	60
Assistant Secretary of the Army (R&D) ATTN: Assistant for Research Washington, D. C. 20301	1
Chief of Naval Research Washington, D. C. 20360	1
Commander, Naval Supply Systems Command (0421G) Department of the Navy Washington, D. C. 20376	1
Commander Naval Facilities Engineering Command Research and Development (Code 0322C) Department of the Navy Washington, D. C. 20390	1
Defense Technical Information Center Cameron Station Alexandria, Virginia 22314	12
Civil Defense Research Project Oak Ridge National Laboratory ATTN: Librarian P. O. Box X Oak Ridge, Tennessee 37830	1
Dr. Eugene P. Wigner Oak Ridge National Laboratory Oak Ridge, Tennessee 37831	1
Mr. Edward L. Hill Research Triangle Institute P. O. Box 12194 Research Triangle Park, North Carolina 27702	2

DISTRIBUTION (Continued)

	No. of Copies
Director, Defense Nuclear Agency ATTN: Mr. David Auton Washington, D. C. 20305	1
Defense Advanced Research Projects Agency 1400 Wilson Boulevard Arlington, Virginia 22209	1
Defense Intelligence Agency (DI-7) Washington, D. C. 20301	1
Department of Energy Technical Information Service Oak Ridge, Tennessee 37830	1
Commanding Officer U. S. Army Combat Developments Command Institute of Nuclear Studies Fort Bliss, Texas 79916	1
Director Lovelace Foundation 5200 Gibson Blvd., S.E. Albuquerque, New Mexico 87108	1
Dr. Walter Wood Dikewood Corporation 1009 Bradbury Drive, S.E. University Research Park Albuquerque, New Mexico 87106	1
Dr. Eugene Sevin 10 West 35th Street Chicago, Illinois 60616	1
Director, U. S. Army Engineer Waterways Experiment Station ATTN: Nuclear Weapons Effects Branch P. O. Box 631 Vicksburg, Mississippi 39180	1

DISTRIBUTION (Continued)

	No. of Copies
Institute for Defense Analysis ATTN: Dr. Leo Schmidt 400 Army-Navy Drive Arlington, Virginia 22202	1
Dr. John Billheimer Systan, Inc. 343 Second Street P. O. Box U Los Altos, California 94022	1
Dr. Conrad Chester Oak Ridge National Laboratory P. O. Box X Oak Ridge, Tennessee 37830	1
Ohio State University Disaster Research Center 127-129 West 10th Avenue Columbus, Ohio 43201	1
Mr. Clark Henderson SRI International, Inc. Menlo Park, California 94025	1
Mr. Carsten M. Haaland Oak Ridge National Laboratory P. O. Box X Oak Ridge, Tennessee 37830	1
Dr. Roger J. Sullivan Systems Planning Corp. 1500 Wilson Boulevard Arlington, Virginia 22209	1
Dr. Lewis V. Spencer Radiation Theory Section 4.3 National Bureau of Standards Washington, D. C. 20234	1

DISTRIBUTION (Continued)

	No. of Copies
Los Alamos Scientific Laboratory ATTN: Document Library Los Alamos, New Mexico 87545	1
Dr. Daniel Willard Office of Operations Research Office of the Under Secretary Department of the Army Washington, D. C. 20301	1
Mr. Anatole Longinow IIT Research Institute 10 West 35th Street Chicago, Illinois 61616	1
Mr. Charles E. Fritz Program Director Contingency Planning and Emergency Services Commission on Sociotechnical Systems National Research Council 2101 Constitution Avenue Washington, D. C. 20418	1
U.S. Air Force Special Weapons Center Kirtland Air Force Base ATTN: Library Albuquerque, New Mexico 87417	1
Dr. Richard Laurino Center for Planning and Research, Inc. 750 Welch Road Palo Alto, California 94304	1
Mr. Walmer E. Strope P. O. Box 1104 Bailey's Crossroads, Virginia 22041	1
Emergency Technology Division Oak Ridge National Laboratory ATTN: Librarian P. O. Box X Oak Ridge, Tennessee 37830	1

DISTRIBUTION (Continued)

	No. of Copies
Chief Engineer ATTN: ENGMC-D Department of the Army Washington, D. C. 20314	1
Army Nuclear Defense Laboratory ATTN: Technical Library Edgewood, Maryland 21010	1
National Academy of Sciences Advisory Committee on Emergency Planning ATTN: Dr. Lauriston Taylor 2101 Constitution Avenue, N.W. Washington, D. C. 20418	1
Dr. Martin O. Cohen Mathematical Applications Group, Inc. 3 Westchester Plaza Elmsford, New York 10523	1
Dr. Charles Eisenhauer National Bureau of Standards Center for Radiation Research Washington, D. C. 20234	1
Assistant Secretary of the Air Force (R&D) Room 4E968, The Pentagon Washington, D. C. 20330	1
Director for Defense Nuclear Agency ATTN: Technical Library Washington, D. C. 20305	1

DEMOGRAPHICS AND CASUALTY PREDICTION/ANALYSIS
(Unclassified)

La Jolla Institute, P. O. Box 1434, La Jolla, CA
February 1980
116 pages
Contract No. DCPA-01-79-C-0244
Work Unit No. 4111C

This report presents a general method of predicting and bounding casualties from both prompt and delayed effects produced by attacks against population. The method contains analytic sub-models for distributions of population and hardness and for nuclear weapons phenomenology.

DEMOGRAPHICS AND CASUALTY PREDICTION/ANALYSIS
(Unclassified)

La Jolla Institute, P. O. Box 1434, La Jolla, CA
February 1980
116 pages
Contract No. DCPA-01-79-C-0244
Work Unit No. 4111C

This report presents a general method of predicting and bounding casualties from both prompt and delayed effects produced by attacks against population. The method contains analytic sub-models for distributions of population and hardness and for nuclear weapons phenomenology.

DEMOGRAPHICS AND CASUALTY PREDICTION/ANALYSIS
(Unclassified)

La Jolla Institute, P. O. Box 1434, La Jolla, CA
February 1980
116 pages
Contract No. DCPA-01-79-C-0244
Work Unit No. 4111C

This report presents a general method of predicting and bounding casualties from both prompt and delayed effects produced by attacks against population. The method contains analytic sub-models for distributions of population and hardness and for nuclear weapons phenomenology.

DEMOGRAPHICS AND CASUALTY PREDICTION/ANALYSIS
(Unclassified)

La Jolla Institute, P. O. Box 1434, La Jolla, CA
February 1980
116 pages
Contract No. DCPA-01-79-C-0244
Work Unit No. 4111C

This report presents a general method of predicting and bounding casualties from both prompt and delayed effects produced by attacks against population. The method contains analytic sub-models for distributions of population and hardness and for nuclear weapons phenomenology.